Hindawi
Oxidative Medicine and Cellular Longevity
Volume 2021, Article ID 5513966, 24 pages
https://doi.org/10.1155/2021/5513966

Research Article

ALKBH5 Exacerbates Aortic Dissection by Promoting Inflammatory Response and Apoptosis of Aortic Smooth Muscle Cells via Regulating lnc-TMPO-AS1/EZH2/IRAK4 Signals in an m6A Modification Manner

Peng Wang,[1,2,3] **Min Zhang**,[1,2] **Zhiwei Wang**,[1,2] **Qi Wu**,[1,2,3] **Feng Shi**,[1,2,3] **and Shun Yuan**[1,2,3]

[1]*Department of Cardiovascular Surgery, Renmin Hospital of Wuhan University, 238# Jiefang Road, Wuhan, 430000 Hubei Province, China*
[2]*Cardiovascular Surgery Laboratory, Renmin Hospital of Wuhan University, 9# Zhangzhidong Road, Wuhan, 430000 Hubei Province, China*
[3]*Central Laboratory, Renmin Hospital of Wuhan University, 9# Zhangzhidong Road, Wuhan, 430000 Hubei Province, China*

Correspondence should be addressed to Zhiwei Wang; wangzhiwei@whu.edu.cn

Received 12 January 2021; Revised 2 March 2021; Accepted 11 March 2021; Published 18 March 2021

Academic Editor: Ciccarelli Michele

Recently, mounting evidence indicates that N6-methyladenosine (m6A) modification functions as a pivotal posttranscriptional modification that regulates noncoding RNA biogenesis to influence the progression of multiple diseases. However, whether m6A modification is involved in aortic dissection (AD) development has never been reported. Meanwhile, numerous studies have shown that AngII-induced inflammatory damage and excessive apoptosis of human aortic smooth muscle cells (HASMCs) are the crucial pathological features of AD development. Therefore, in this study, we intended to explore whether m6A modification can regulate AD progression by influencing the damage effects of AngII on HASMCs and elucidate the underlying mechanisms. Firstly, we screened and confirmed the high expression of alkylation repair homolog protein 5 (ALKBH5), a key m6A demethylase, in aortic tissues from AD patients, indicating that m6A modification may indeed be involved in AD progression. Subsequently, we demonstrated that ALKBH5 can exacerbate the AngII-induced HASMC inflammatory injury as well as apoptosis and shorten the survival time of AngII-infused mice. Mechanistically, we revealed that lncRNA TMPO-AS1 is a downstream target for ALKBH5 to affect AD progression in vitro and vivo. Meanwhile, we confirmed that ALKBH5-mediated m6A demethylation downregulates lnc-TMPO-AS1 by decreasing the stability of its nascent. Further, we demonstrated that lnc-TMPO-AS1 exhibits its functions in HASMCs, at least partly, through downregulating IRAK4 at the epigenetic level by combining with EZH2. Finally, the direct positive correlation between ALKBH5 and IRAK4 in terms of the expression level and biological function was confirmed, which further enforced the preciseness and correctness of our findings. In conclusion, our study demonstrated that ALKBH5 aggravates AD by promoting inflammatory response and apoptosis of HASMCs via regulating lnc-TMPO-AS1/EZH2/IRAK4 signals in an m6A modification manner and may provide a novel molecular basis for subsequent researchers to searching for novel therapeutic approaches to improve the health of patients fighting AD and other cardiovascular diseases.

1. Introduction

Aortic dissection (AD) is a life-threatening cardiovascular emergency due to a tear in the aorta intima or bleeding within the aortic wall, leading to the separation of the different layers of the aortic wall [1, 2]. One of the first prerequisites to explore new therapeutic strategies for AD is to elucidate the potential molecular mechanisms involved.

Numerous studies have shown that inflammatory damage and excessive apoptosis of human aortic smooth muscle

cells (HASMCs) are the crucial pathological features of AD development [3–5]. Meanwhile, our previous study has demonstrated that treating ASMCs with a certain concentration of angiotensin II (AngII) can simulate the status of cellular injury during the development of AD in the physiological state [6]. Therefore, in the present study, we intended to identify some signaling molecules that could regulate AD progression by influencing the damage effects of AngII on HASMCs and clarify their mechanisms of action.

The dysfunction of HASMCs is a complex biological process caused by epigenetic abnormalities and/or abnormal genetic variations. Epigenetic abnormalities mainly occur at the following levels: histone modification [7], DNA [8], and RNA [9]. In RNA levels, over 100 types of RNA modifications have been identified, among which N6-methyladenosine (m6A) RNA methylation is the most common modification in eukaryotes [10–12]. Moreover, m6A modification is demonstrated by many studies to be a dynamic and reversible process, constructed primarily by a methyltransferase complex called m6A "writers," including methyltransferase like 3 (METTL3), vir-like methyltransferase (VIRMA), coupled with WT1-associated protein (WTAP) and removed by demethylases called m6A "erasers," including alkylation repair homolog protein 5 (ALKBH5) and fat mass and obesity-associated protein (FTO) [13, 14].

Recently, increasing evidence also revealed that m6A modification functions as a pivotal posttranscriptional modification that regulates mRNA and noncoding RNA biogenesis to influence the progression of multiple diseases; for instance, Lin et al. demonstrated that METTL3 could facilitate lung cancer development by promoting translation initiation of many oncogenes through m6A modification [15]. Lan et al. reported that VIRMA could contribute to liver cancer progression by causing the separation of the RNA-binding protein HuR and the degradation of GATA3 pre-mRNA in an m6A modification manner [16]. Zhang et al. found that ALKBH5 could promote invasion and metastasis of gastric cancer via decreasing methylation of the lncRNA NEAT1 [17]. However, whether m6A modification is involved and whether it acts by regulating noncoding RNAs in the development of AD has never been reported.

In the present study, we confirmed that ALKBH5 was highly expressed in AD tissues as well as HASMCs treated with AngII and could exacerbate AngII-induced HASMC inflammation and apoptosis in vitro. Moreover, overexpressing ALKBH5 increased the incidence of AD in AngII-infused mice and shorten their survival time. Mechanistically, ALKBH5-mediated m6A demethylation induced the downregulation of long noncoding RNA (lncRNA) TMPO-AS1 by reducing the stability of nascent lnc-TMPO-AS1, which subsequently enhanced the expression of IRAK4 by decreasing binding to EZH2 at the epigenetic level. Collectively, our findings provided a novel insight into the role of m6A modification in the onset and progression of AD.

2. Materials and Methods

2.1. Clinical Samples. Aortic media samples ($n = 40$) were obtained from acute thoracic AD patients who underwent emergency aortic replacement surgery from May 2016 to November 2019. Patients enrolled in our study were confirmed to have no connective tissue diseases, such as Marfan syndrome and Ehlers-Danlos syndrome, or a family history of aortic diseases. Meanwhile, normal aorta tissues ($n = 40$) were collected from heart donors declared brain dead. Both the informed written consent of all participants and the approval of the Clinical Research Ethics Committees of Renmin Hospital of Wuhan University for the collection and usage of clinical specimens were obtained. The baseline characteristics of the AD patients and aortic donors are presented in Supplementary Table 1.

2.2. Cell Culture and Liposome Transfection. HASMCs were purchased from ATCC (PCS-100-012™) and incubated in DMEM (HyClone, UT) containing 10% fetal bovine serum (FBS; Invitrogen) and 1% penicillin/streptomycin (Sigma). The external conditions for cell culture were as follows: 37°C, humidified atmosphere containing 5% CO_2. As previously reported, we established the cell model simulating the damaged state of HASMCs during AD in the present study by treating HASMCs with 0.1 μM AngII for 12 h [18].

To obtain stable cell lines, we purchased multiple lentivirus, including ALKBH5 overexpression lentivirus (termed as LV-ALKBH5), a negative control (termed as LV-NC), ALKBH5 knockdown lentivirus (termed as sh-ALKBH5), or scramble control (termed as sh-NC) from GeneChem (Shanghai, China). Lentiviruses were separately transfected into HASMCs when cell confluence attained 60%. Stable cell clones were selected using puromycin (4 μg/ml) for 1 week.

For the overexpression of specific genes, we obtained overexpression plasmids, pcDNA3.1-TMPO-AS1, pcDNA3.1-EZH2, and pcDNA3.1-IRAK4, from GeneChem Co., Ltd. (Shanghai, China). Meanwhile, we commissioned RiboBio Co., Ltd. to synthesize small interfering RNA (siRNA) to specifically target sequences in TMPO-AS1 (si-TMPO-AS1), EZH2 (si-EZH2), and IRAK4 (si-IRAK4). The pcDNA3.1 empty vector (pcDNA-NC) or si-scr-RNA (si-NC) was their respective negative control. HASMCs were randomly transiently transfected with one of the plasmids or siRNAs using Lipofectamine 3000 (Invitrogen, USA).

2.3. AngII Infusion AD Model and Adenovirus Vector Transfection. The animal experiments were approved by the Ethical Committee of the Renmin Hospital of Wuhan University and performed following the Current Guidelines for the Care and Use of Laboratory Animals published by the National Institutes of Health. Male C57BL/6N mice were purchased from the Guangdong Medical Laboratory Animal Center (Foshan, China). All mice were in a pathogen-free environment with proper temperature (22°C) as well as humidity (60–65%) and given a normal chow diet and water.

The angiotensin II (AngII) infusion mouse AD model was constructed as described in a previous study [19]. Concretely, osmotic minipumps (ALZET, USA) containing AngII (1 μg/kg/min, Enzo Life Sciences, USA) were implanted in eight-week-old male C57BL/6N mice. All mice were monitored daily to record their survival time and death reasons. The experimental endpoint was mouse death from

aortic rupture or treatment time up to 28 days. Whether they died within 28 days or were euthanized on the 28th day, the aortas were collected to confirm the formation of AD.

To interfere with ALKBH5 level in vivo, adeno-associated virus 9 (AAV9) that can transfect the aorta tissue was used in the present study. 1×10^{12} viral genome particles carrying different plasmids and interfering RNAs in 100 μl of saline were randomly injected through the tail vein of C57BL/6N mice.

2.4. RNA Extraction and qRT-PCR Analyses. Total RNA was extracted from tissues and cells via using TRIzol Reagent (Invitrogen, USA). Then, samples with OD value greater than 1.9 were reverse transcribed to cDNA by utilizing the Super-Script III Reverse Transcriptase kit (Invitrogen). Quantitative real-time PCR (qRT-PCR) was performed on the Applied Biosystems™ 7500 Real-Time PCR System using Fast SYBR Green Master Mix Kit (Applied Biosystems, USA). The relative expression level mRNA was evaluated using the $2^{-\Delta\Delta Ct}$ method and normalized to their corresponding internal control, U6 snRNA, or β-actin. All primers were designed and synthesized by RiboBio Co. (Guangzhou, China).

2.5. Western Blot. Tissue specimens or cells were lysed by RIPA lysis buffer containing 1% protease inhibitors (Sigma, USA). The protein extractions were quantified by BCA Protein Assay Kit (Beyotime, China). Equivalent protein samples (25 μg) were electrophoretically separated on 10% SDS-PAGE and then transferred to polyvinylidene difluoride membrane (PVDF). After being blocked in 5% skim milk, PVDFs were incubated with monoclonal primary antibodies, including anti-ALKBH5 (ab69325; Abcam), anti-EZH2 (#5246; Cell Signaling Technology), anti-IRAK4 (ab32511; Abcam), anti- pNFκB (ab32536; Abcam), and anti-GAPDH (ab9485; Abcam) at 4°C overnight. Next, the membranes were incubated with a peroxidase-conjugated secondary antibody. The western blot bands were visualized by Pierce™ ECL (Thermo Fisher Scientific Inc., USA) and analyzed using ImageJ software [20].

2.6. Enzyme-Linked Immunosorbent Assay (ELISA). The levels of inflammatory factors (IL-1β, IL-6, IL-17A, and TNF-α) in the culture medium supernatants of HASMCs treated or untreated with AngII were measured by ELISA kits (R&D, MN, USA). The OD value at 450 nm wavelength was detected by Infinite F50® microplate reader (Tecan, CH).

2.7. TUNEL Assay. HASMCs were fixed in paraformaldehyde for 15 min and stained by In Situ Cell Death Detection Kit (TMR red) (Roche, Switzerland). Six visual fields were randomly chosen from each group to calculate the positive TUNEL-stained cells which were visualized with a fluorescence microscope (BX63, Olympus, Japan).

2.8. Flow Cytometry. Each group of HASMCs was collected, resuspended, and double-stained with Annexin V-FITC (556547, BD), coupled with propidium iodide (PI; Solarbio, China) at room temperature for 10 min in darkness. Subsequently, cell apoptosis was analyzed within 1 h using the FACScan flow cytometer installed with Cell Quest software (BD Biosciences, USA).

2.9. Microarray Analysis. To obtain the lncRNA expression profiling in aorta tissues for further hierarchical clustering analysis, a microarray analysis was performed on Human lncRNA Array v4.0 (8 × 60 K, Arraystar, USA) and its results were analyzed by using R software with related packages.

2.10. RNA m6A Dot Blots. The poly(A)$^+$ RNAs (100 and 250 ng, respectively) were denatured by heating at 65°C for 5 min and spotted onto a nylon membrane (Sigma, USA) with a Bio-Dot apparatus (Bio-Rad, USA). The membranes were ultraviolet (UV) crosslinked, blocked, incubated with m6A antibody (1 :20091000, Synaptic Systems, #202003) overnight at 4°C, and then incubated with HRP-conjugated anti-mouse IgG (1 : 5000, Proteintech, USA). After extensive washing, membranes were visualized by the chemiluminescence system (Bio-Rad, USA). The membrane stained with 0.02% methylene blue (MB) in 0.3 M sodium acetate (pH 5.2) was used to ensure consistency between groups.

2.11. Chromatin Immunoprecipitation (ChIP) Assay. ChIP assay was performed according to the manufacturer's manual (Millipore, USA) as described previously [13]. The specific antibodies for H3 trimethyl-Lys-27 or EZH2 were purchased from Millipore.

2.12. RNA Immunoprecipitation (RIP) Assay. RIP assay was conducted using Magna RIP™ RNA-Binding Protein Immunoprecipitation Kit (Millipore, USA). After HASMCs were lysed and centrifuged, the supernatant was incubated with magnetic beads conjugated with antibodies against Argonaute-2 (anti-Ago2), m6A (anti-m6A), or anti-Immunoglobulin G (anti-IgG) at 4°C overnight. The precipitated RNAs were eluted, purified, and then examined by qRT-PCR.

2.13. Subcellular Fractionation Analysis. Cytoplasmic and Nuclear RNA Purification Kit (Cat. 21000; Norgen, Canada) was utilized for subcellular isolation of RNAs in HASMCs. The fractions of cytoplasmic and nuclear were detected by qRT-PCR, with GAPDH and U6 serving as their internal references, respectively.

2.14. Immunofluorescence and Fluorescence In Situ Hybridization (FISH). HASMCs were fixed in PBS containing 4% paraformaldehyde for 10 min at room temperature and permeabilized in PBS containing 0.1% Triton-X as well as 1% BSA at room temperature for 30 min. DNA staining was conducted with DAPI. EZH2 (Bioss) was detected with an anti-EZH2 antibody for approximately 16 h (37°C). Specific FISH probes to lncRNA TMPO-AS1 were designed and synthesized by RiboBio Co. (Guangzhou, China). The hybridization was performed in HASMCs as previously reported [12]. Imaging was performed on a confocal laser scanning microscope (Leica Microsystems, Mannheim, Germany).

2.15. mRNA Stability Detection. To detect the influence of ALKBH5 on the half-life of lnc-TMPO-AS1, we treated HASMCs with 5 μg/ml actinomycin D (Act-D) (#A9415, Sigma, USA). After incubation at the indicated times, the

total RNA of cells was extracted for qRT-PCR. The mRNA half-life of lnc-TMPO-AS1 was calculated using ln2/slope, with GAPDH being used for normalization.

2.16. HE Staining. Resected aorta samples from the normal and AD mice were fixed in 4% formaldehyde overnight, dehydrated, paraffin-embedded, and cut into 4 μm thick sections. The tissue sections were stained with hematoxylin and eosin (HE). Then, the samples were placed under a microscope and photographed at 100x and 400x fields of view as previously described [21].

2.17. Statistical Analysis. All statistical analyses were performed by using SPSS 24.0 (IBM Co., USA) and GraphPad Prism 8.0 (GraphPad Software, USA). Two-tailed Student's *t*-test and Pearson's correlation coefficient analysis were, respectively, adopted to analyze differences between groups or the correlations between ALKBH5, lncRNA, TMPO-AS1, EZH2, and IRAK4. Kaplan-Meier curve with the log-rank test was used to compare the survival time. A two-sided P value < 0.05 was considered statistically significant. Each experiment was performed in triplicate, and all data are presented as mean ± standard error of the mean (SEM).

3. Results

3.1. ALKBH5 Is Upregulated in AD Tissues and HASMCs Treated with AngII. In recent years, more and more evidence confirmed that m6A methylation modification acts a crucial role in various biological processes. However, hardly any studies have been conducted in AD [1, 2]. In the present study, to determine whether m6A modification participates in AD progress, the expression levels of multiple key genes involved in m6A modification, as enumerated in Section 1, were measured in 40 pairs of AD and normal arterial tissues. Higher levels of ALKBH5 and lower levels of KIAA1429 were confirmed in AD tissues compared with normal arterial tissues (Figure 1(a)). The results of western blot also revealed the low expression of KIAA1429 and the high expression of ALKBH5 in aortic tissues from AD patients compared with donors (Figure 1(b); Supplementary Fig. 1). The same results emerged when we detected their expression level in 20 pairs of normal and diseased aorta samples from the normal and AngII-induced AD mice by qRT-PCR and western blot (Figures 1(c) and 1(d); Supplementary Fig. 2). Moreover, we also detected ALKBH5 and KIAA1429 levels in HASMCs untreated and treated with AngII; as described in Section 2, the results consistent with the trends measured in tissues appearing (Figures 1(e) and 1(f)). Given the more drastic changes in the mRNA expression level of ALKBH5, we chose it as the research object of this study. Taken together, the aberrant expression of ALKBH5 in AD tissues derived from humans and mice and HASMCs treated with AngII was verified, suggesting that m6A modification might be indeed involved in the development of AD.

3.2. ALKBH5 Exacerbates AngII-Induced Inflammatory Response and Apoptosis of HASMCs and Increases the Incidence of AD in AngII-Infused Mice. To investigate the biological function of m6A modification in HASMCs, we overexpressed or knocked down ALKBH5, a vital m6A demethylase exhibiting a negative correlation with m6A levels, via transfection with LV-ALKBH5 and sh-ALKBH5 in HASMCs, respectively. The interference effects of transfection were detected by qRT-PCR and western blot (Figures 2(a) and 2(b)). Subsequently, we first measured the levels of proinflammatory mediators in the supernatant of the cell culture medium using ELISA. The results showed that the secretion of inflammatory cytokines, including IL-1β, IL-6, IL-17A, and TNF-α, were greatly elevated in the AngII-treated groups. Meanwhile, the overexpression of ALKBH5 evidently enhanced the promoting effect of AngII on their secretion (Figures 2(c)–2(f)). On the contrary, we also found that ALKBH5 knockdown could suppress the expression of the genes corresponding to the aforesaid inflammatory factors in HASMCs by using qRT-PCR (Figures 2(g)–2(j)). Furthermore, nuclear factor kappa B (NFκB) is a key regulator of immune development, immune responses, and inflammation. Its activation leads to the activation of associated inflammatory pathways, and the level of phosphorylation of NFκB (pNFκB) in cells can reflect the level at which it is activated [22]. Herein, we investigated the influence of ALKBH5 on the levels of pNFκB. The result showed that the expression of pNFκB was upregulated in the AngII-treated group and ALKBH5 significantly enhanced the promoting effect of AngII on it (Figure 2(k); Supplementary Fig. 3). Next, we performed TUNEL assay and observed that AngII could induce apoptosis of HASMCs. Moreover, this effect was significantly enhanced when ALKBH5 was overexpressed and weakened when it is silenced (Figure 2(l); Supplementary Fig. 4).

To further examine whether ALKBH5 affects AD progression in vivo, after 28 days of AngII infusion, we observed the incidence of AD and the survival time of mice in multiple groups that received different AAV9 injections. The results revealed that AngII could significantly increase the incidence of AD, and this impact was significantly enhanced by the overexpression of ALKBH5 and reduced by its knockdown (Figure 2(m)). Consistent with the above trends, mice in the AngII+LV-ALKBH5 group and AngII+sh-ALKBH5 group had the shortest and longest lifespans, respectively (Figure 2(n)). In this study, we confirmed whether the mice had AD through gross observation and HE staining of histological observation of their aortic tissue. Gross observations showed that the aorta of AD mice was significantly congested and thickened, and histological observations confirmed the destruction of aortic tissue and the formation of AD (Figures 2(o) and 2(p)). Collectively, our findings revealed that ALKBH5 can exacerbate AngII-induced inflammatory response and apoptosis of HASMCs, as well as the progression of AD in vivo.

3.3. lncRNA TMPO-AS1 Is a Downstream Target of ALKBH5. Two previous studies have confirmed that METTL3, a key methylase upregulating m6A levels, can affect cellular function by regulating specific downstream lncRNA in cancer [3, 4]. We herein identified whether ALKBH5 also functions in HASMCs via modulating its target lncRNAs. Firstly, through using lncRNA microarrays, we obtained lncRNA

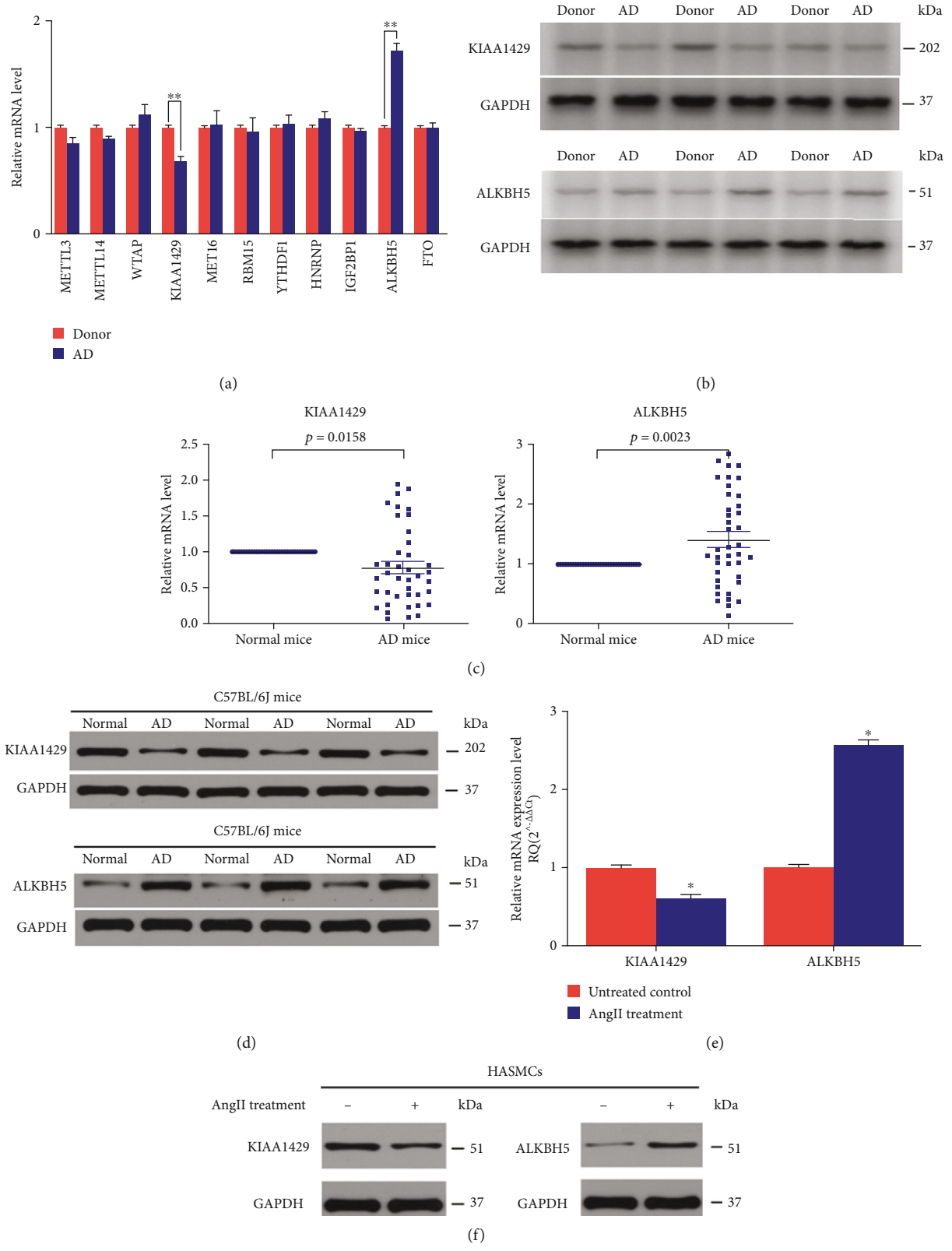

Figure 1: ALKBH5 is upregulated in AD tissues and HASMCs treated with AngII. (a) The expression levels of multiple key genes related to m6A modification were measured in 40 pairs of the AD and normal arterial tissues. (b) The results of western blot also revealed the low expression of KIAA1429 and the high expression of ALKBH5 in aortic tissues from AD patients. (c, d) The results of western blot also revealed the low expression of KIAA1429 and the high expression of ALKBH5 in aortic tissues from AD mice compared with normal mice. (e, f) The results of western blot also revealed the low expression of KIAA1429 and the high expression of ALKBH5 in HASMCs treated with AngII. Data represented the mean ± SEM from three independent experiments, $^{*}P < 0.05$, $^{**}P < 0.01$.

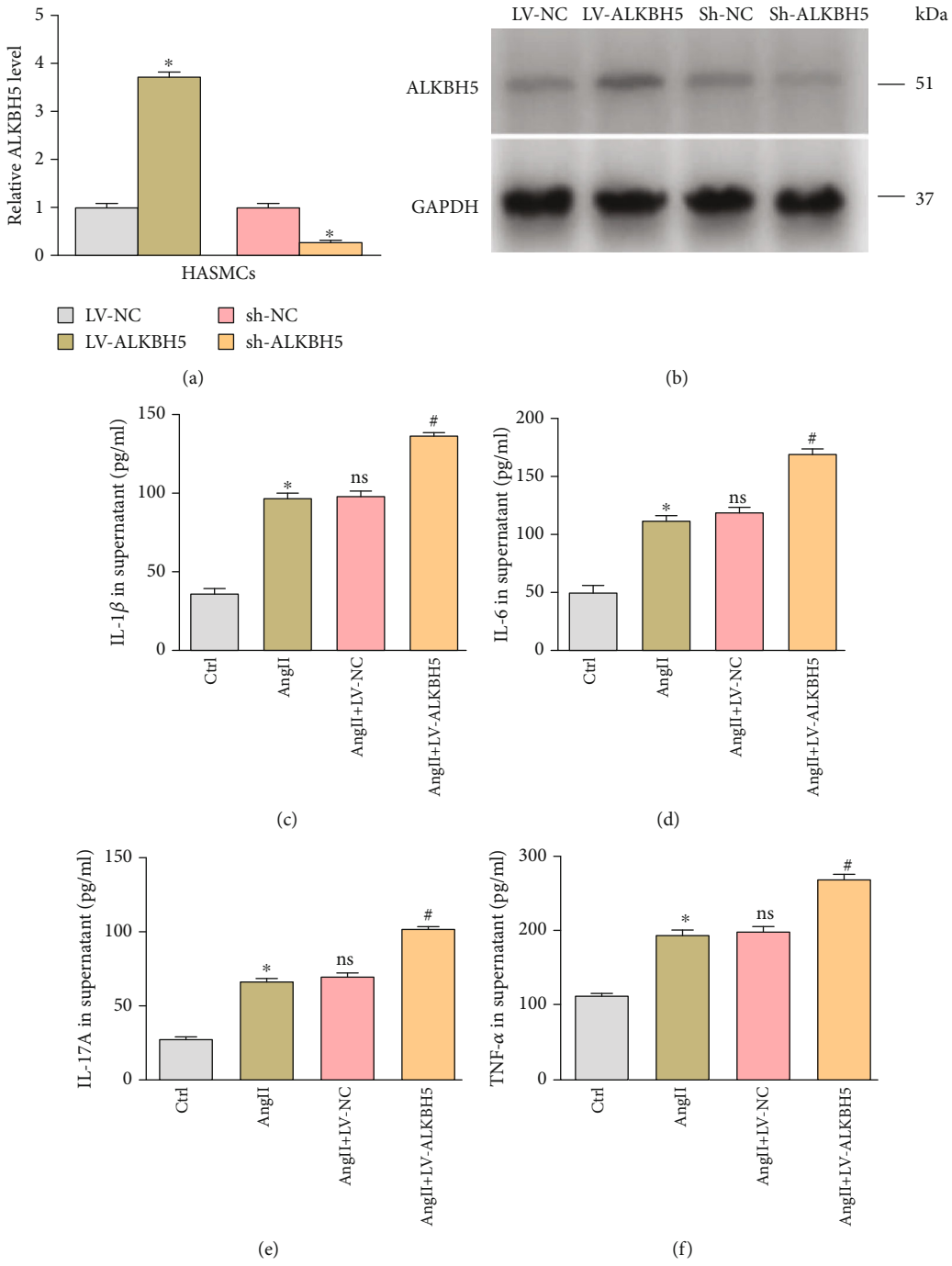

Figure 2: Continued.

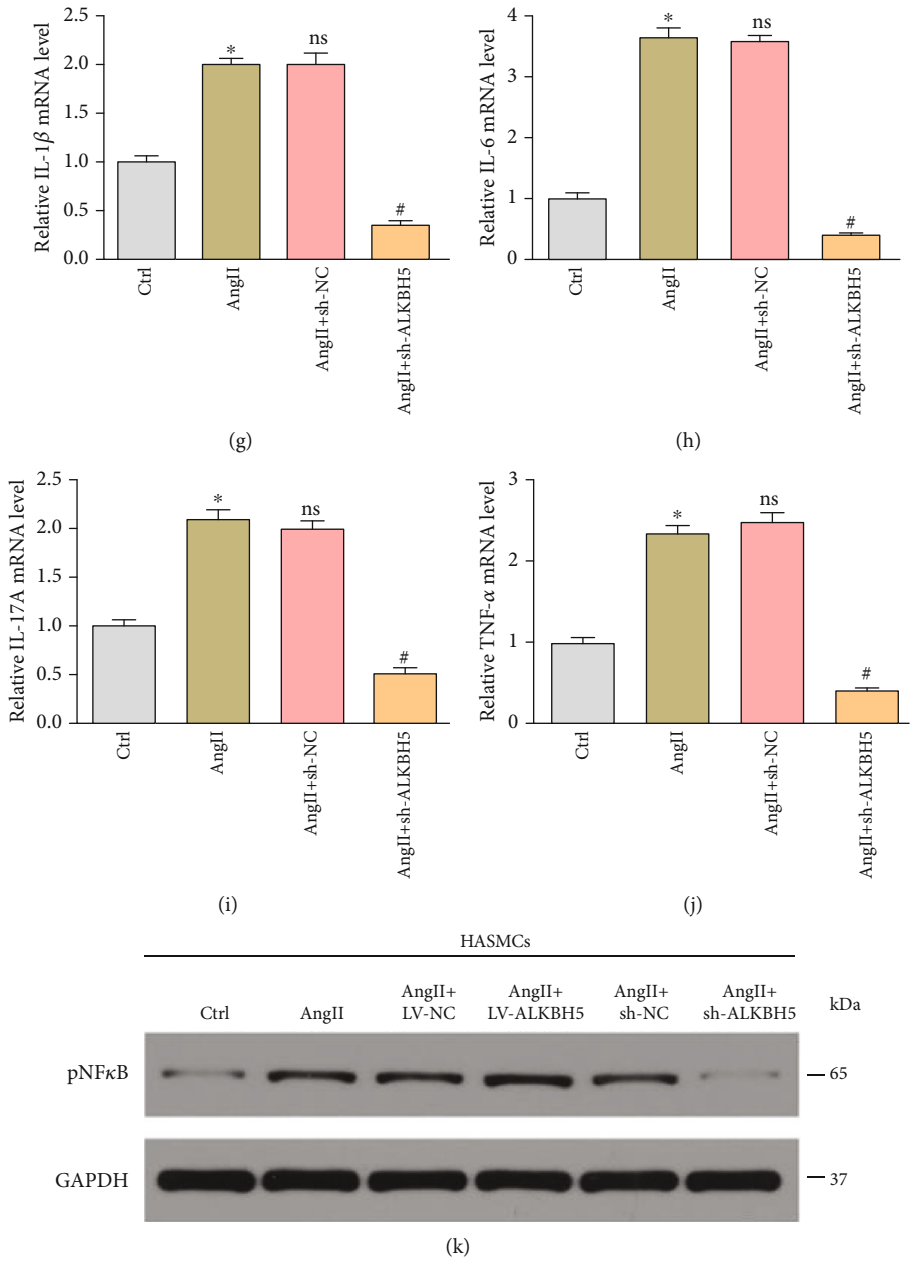

Figure 2: Continued.

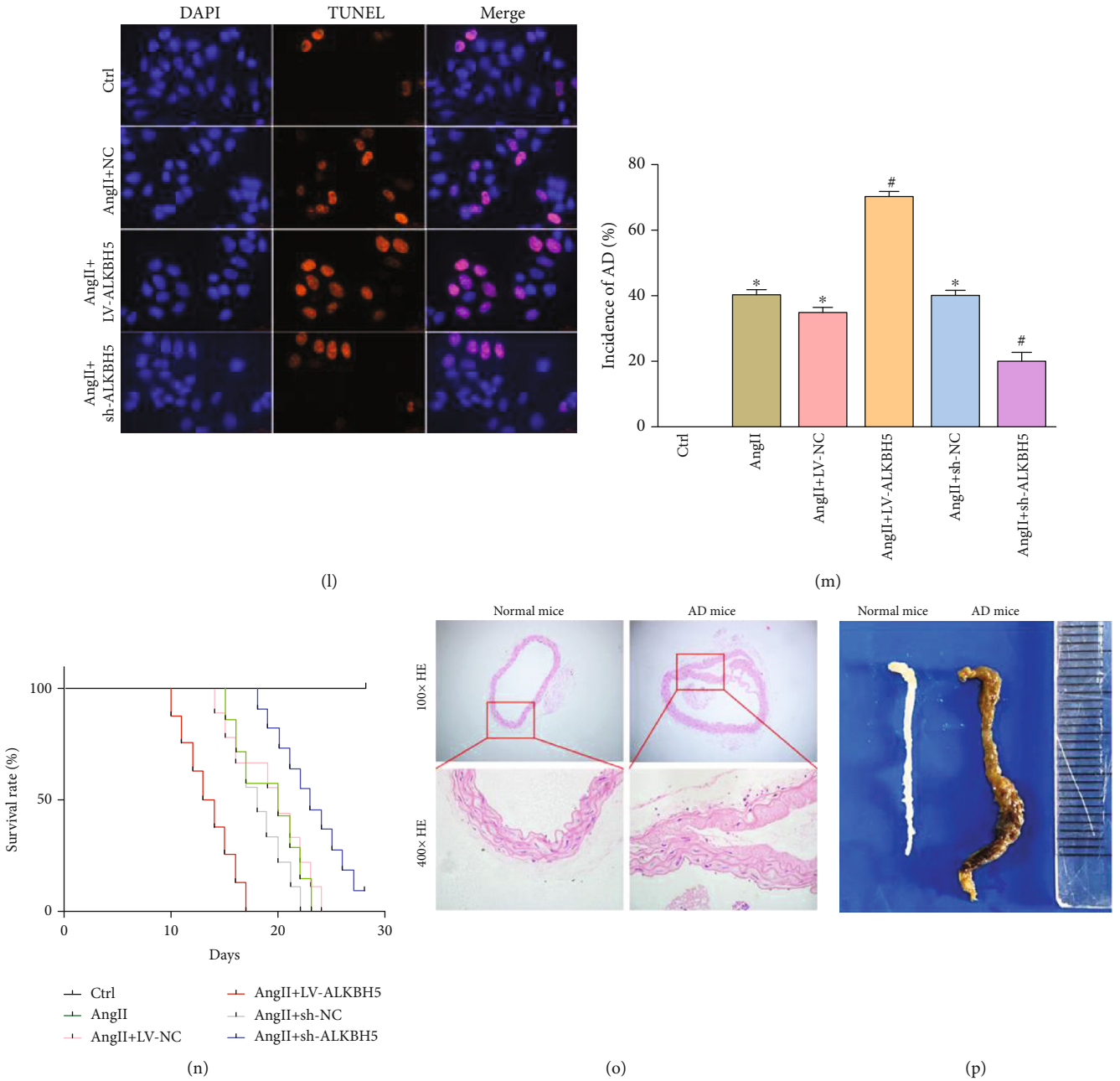

Figure 2: ALKBH5 exacerbates AngII-induced inflammatory response and apoptosis of HASMCs and increases the incidence of AD in AngII-infused mice. (a, b) The interference effects of LV-ALKBH5 and sh-ALKBH5 on ALKBH5 expression in HASMCs were detected by qRT-PCR and western blot. (c–f) The overexpression of ALKBH5 evidently enhanced the promoting effect of AngII on the secretion of inflammatory cytokines in HASMCs. (g–j) ALKBH5 knockdown could suppress the expression of the genes corresponding to the aforesaid inflammatory factors in HASMCs. (k) The expression of pNFκB was upregulated in the AngII-treated group and ALKBH5 significantly enhanced the promoting effect of AngII on it. (l) AngII could induce HASMC apoptosis, and this effect was significantly enhanced when ALKBH5 was overexpressed and weakened when it is silenced. (m) AngII could significantly increase the incidence of AD, and this impact was significantly enhanced by the overexpression of ALKBH5 and reduced by its knockdown. (n) Mice in the AngII +LV-ALKBH5 group and AngII+sh-ALKBH5 group had the shortest and longest lifespans, respectively. (o, p) Gross observations showed that the aorta of AD mice was significantly congested and thickened, and histological observations confirmed the destruction of aortic tissue and the formation of AD. Data represented the mean ± SEM from three independent experiments, $^{*}P < 0.05$ versus the Ctrl group; $^{\#}P < 0.05$ versus the AngII+ LV-NC/sh-NC group; $^{ns}P > 0.05$ versus the AngII group.

expression profiles in aorta tissues from AD patients or donors and observed that 508 lncRNAs in AD specimens showed distinct fold changes, among which 282 were down-regulated and 226 upregulated (fold change < 0.5 or >1.8, $P < 0.05$). In combination with the bioinformatics analysis and literature review, from the above differentially expressed lncRNAs, 40 candidate lncRNAs that may be involved in AD progression were selected for hierarchical clustering

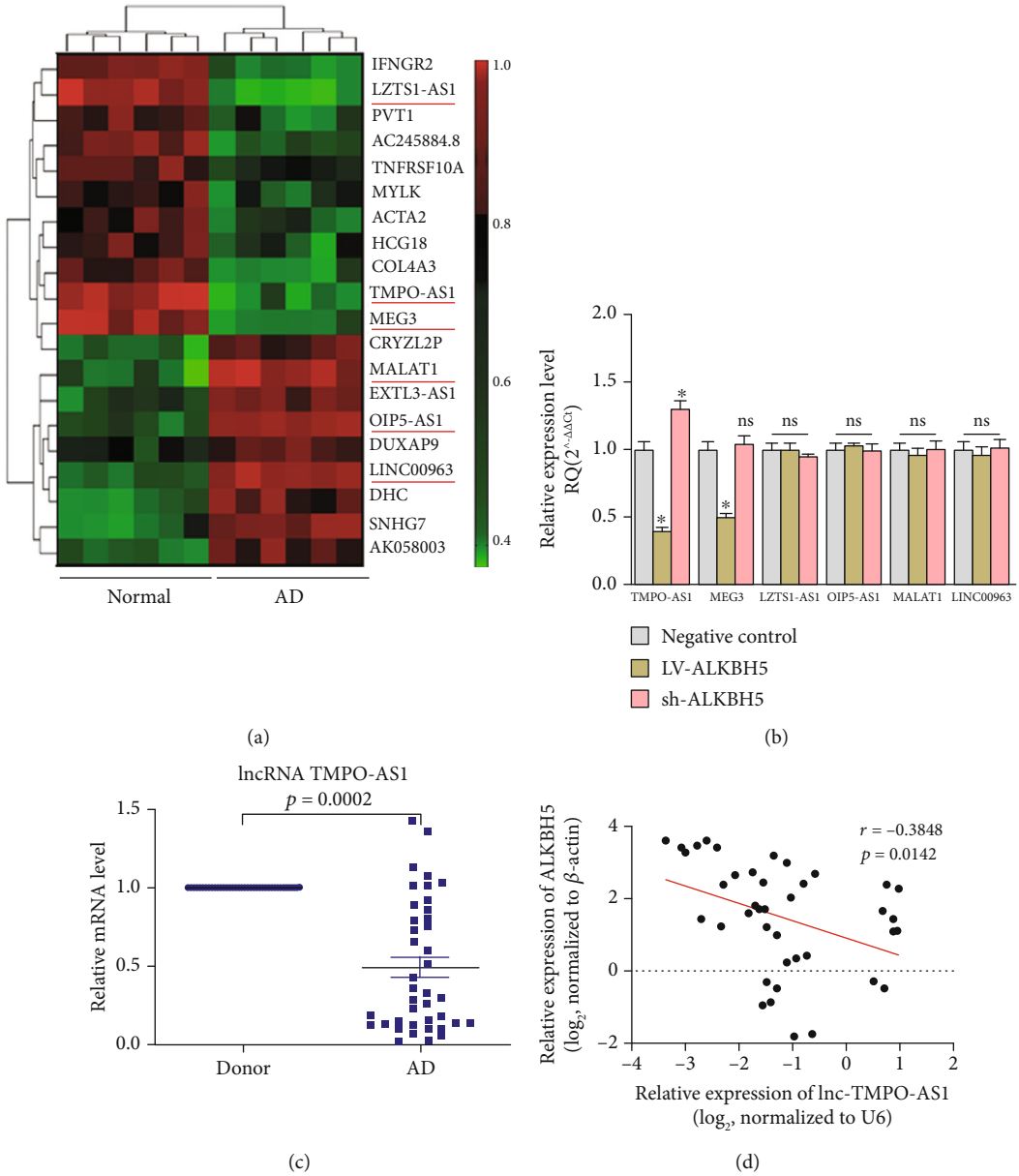

Figure 3: Continued.

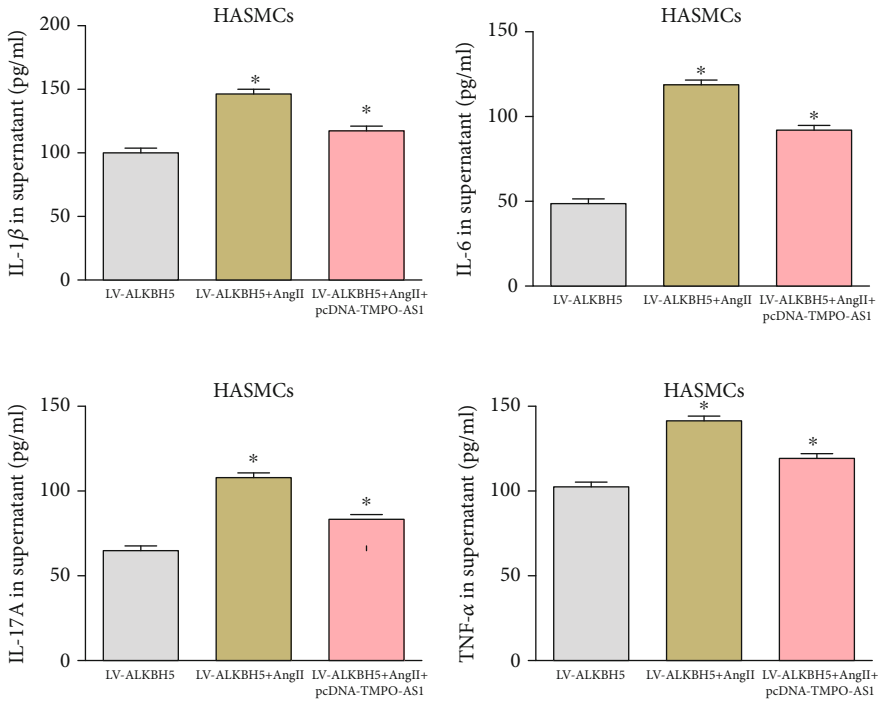

(e)

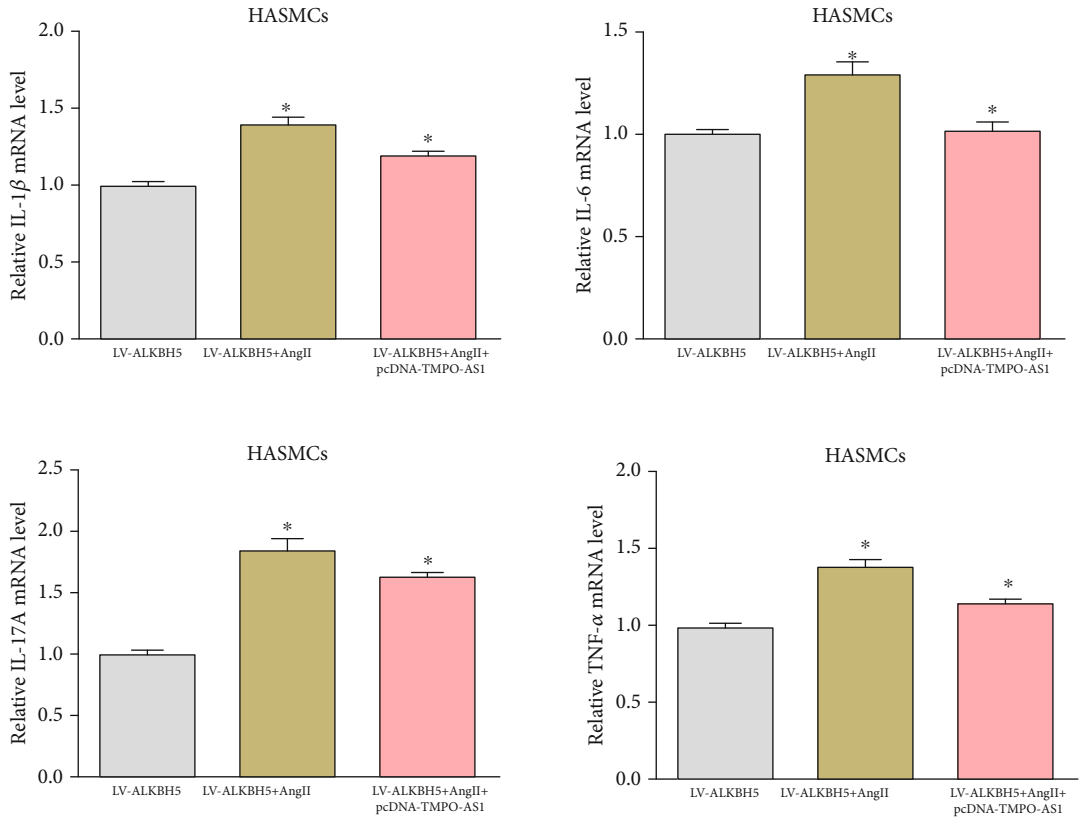

(f)

Figure 3: Continued.

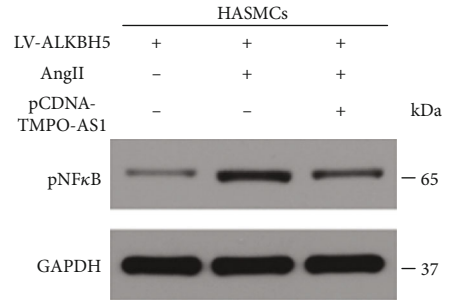

(g)

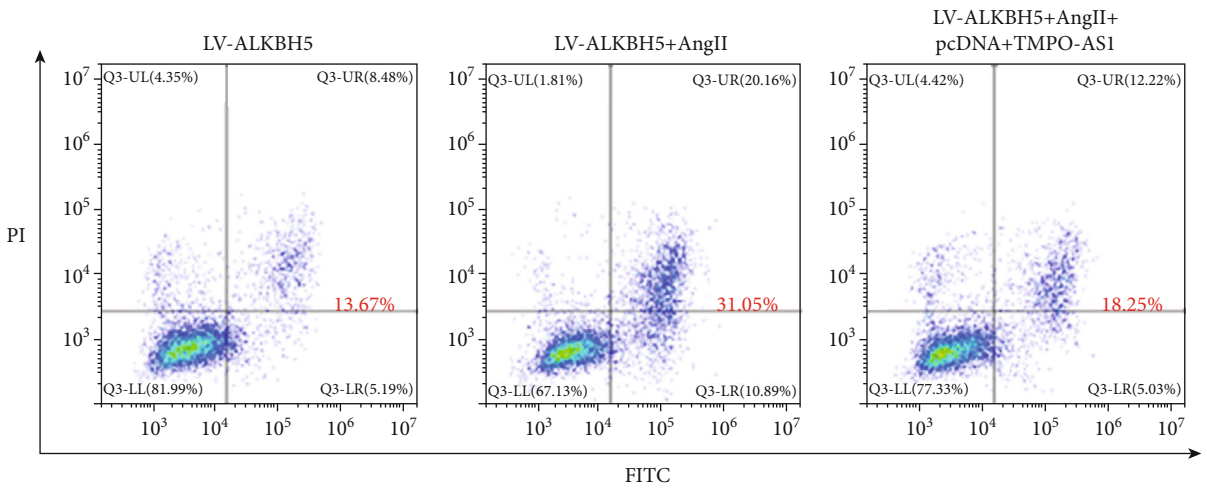

(h)

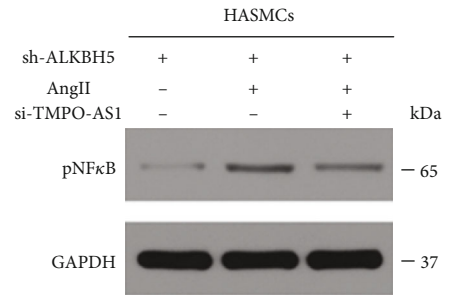

(i)

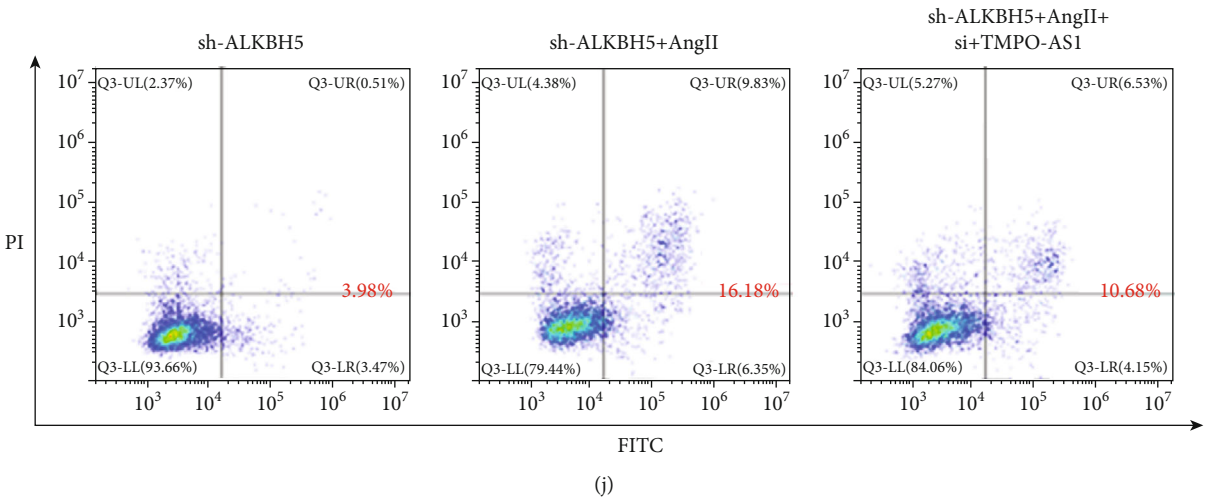

(j)

Figure 3: Continued.

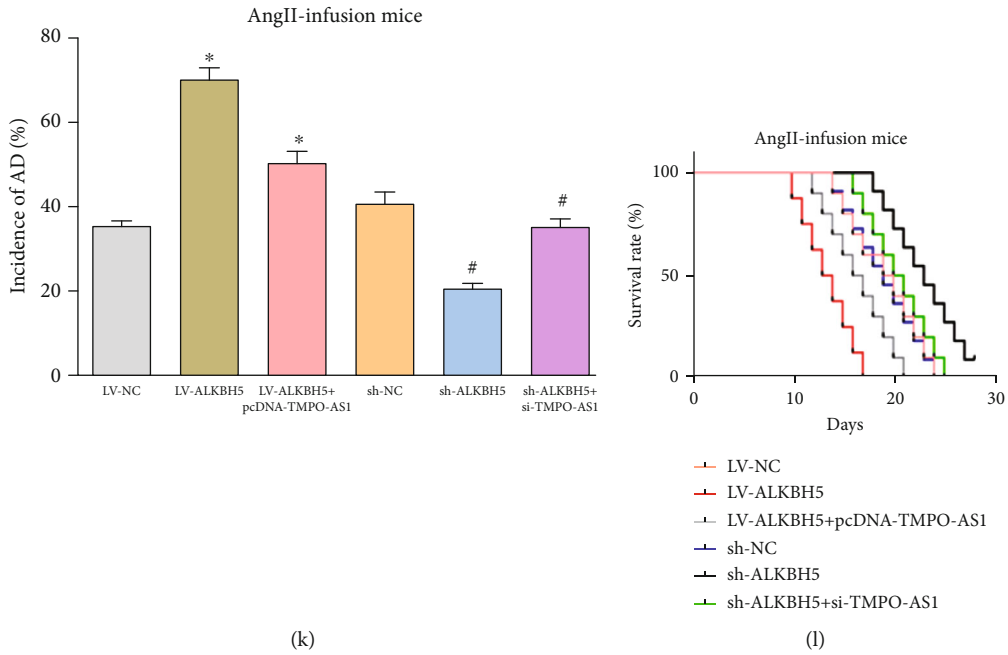

Figure 3: lncRNA TMPO-AS1 is a downstream target of ALKBH5. (a) 40 candidate lncRNAs that may be involved in AD progression were selected for hierarchical clustering analysis. (b) Only the expression of lnc-TMPO-AS1 was altered when ALKBH5 was either overexpressed or silenced. (c, d) The low expression of lnc-TMPO-AS1 in clinical samples and the significantly negative correlation between it and ALKBH5 were confirmed by qRT-PCR and Pearson's correlation coefficient analysis, respectively ($r = -0.438$, $P = 0.043$). (e–h) lnc-TMPO-AS1 upregulation could partly weaken the promoting effect of ALKBH5 overexpression on AngII-induced inflammatory response and apoptosis of HASMCs. (i, j) Downregulation of lnc-TMPO-AS1 could partly reverse the impact of ALKBH5 knockdown on the apoptosis of HASMCs induced by AngII. (k) lnc-TMPO-AS1 upregulation could partly reduce the stimulating effect of ALKBH5 overexpression on the incidence of AD in AngII-infused mice, while its knockdown could partly counteract the impact of ALKBH5 knockdown on this index. (l) lnc-TMPO-AS1 could prolong the survival time of mice and partly counteract the effect of ALKBH5. Data represented the mean ± SEM from three independent experiments, $^*P < 0.05$; ns represents no statistical difference between groups.

analysis (Figure 3(a)). Next, we chose several of these lncRNAs with the most significant changes and determined the variations in their expression levels when ALKBH5 was overexpressed or silenced in cells. The results showed that lncRNA TMPO-AS1 and MEG3 were remarkably downregulated after ALKBH5 overexpression. However, when ALKBH5 was silenced, only the expression of lncRNA TMPO-AS1 was markedly enhanced (Figure 3(b)). Based on this, we chose lnc-TMPO-AS1 for the following study. At the tissue level, its low expression in clinical samples and the significantly negative correlation between it and ALKBH5 were confirmed by qRT-PCR and Pearson's correlation coefficient analysis, respectively (Figures 3(c) and 3(d); $r = -0.438$, $P = 0.043$).

To explore the biological function of lnc-TMPO-AS1 in AD progression as a downstream target of ALKBH5, we first upregulated lnc-TMPO-AS1 in stable ALKBH5-overpressing HASMCs (Supplementary Fig. 5A) and observed that its upregulation could partly weaken the promoting effect of ALKBH5 overexpression on AngII-induced inflammatory response and apoptosis of HASMCs (Figures 3(e)–3(h); Supplementary Fig. 6A). Consistently, when we silenced lnc-TMPO-AS1 in stable ALKBH5-deleting HASMCs (Supplementary Fig. 5B), we found that the downregulation of lnc-TMPO-AS1 could partly reverse the impact of ALKBH5 knockdown on the inflammatory response and apoptosis of HASMCs induced by AngII (Figures 3(i) and 3(j); Supplementary Fig. 6B and 7).

To further elucidate the influence of lnc-TMPO-AS1 on AD development as a downstream effector of ALKBH5 in vivo, we implemented a gene-interference-function study in AngII-infused C57BL/6N mice. First, 1×10^{12} viral genome particles of adeno-associated virus 9 (AAV9), including AAV9-LV-NC, AAV9-LV-ALKBH5, AAV9-LV-ALKBH5/pcDNA-TMPO-AS1, AAV9-sh-NC, AAV9-sh-ALKBH5, or AAV9-sh-ALKBH5/si-TMPO-AS1 in 100 μl of saline were randomly injected through the tail vein to C57BL/6N mice. At 28 days after AngII infusion, the incidence of AD and the survival time of mice in multiple groups were counted and analyzed. The results indicated that lnc-TMPO-AS1 upregulation could partly reduce the stimulating effect of ALKBH5 overexpression on the incidence of AD in AngII-infused mice, while its knockdown could partly counteract the impact of ALKBH5 knockdown on this index (Figure 3(k)). Consistent with the above results, lnc-TMPO-AS1 could prolong the survival time of mice and partly counteract the effect of ALKBH5 (Figure 3(l)). Taken together, our findings revealed that lnc-MPO-AS1 is a downstream target for ALKBH5 to exert its influence on AD progression in vitro and vivo.

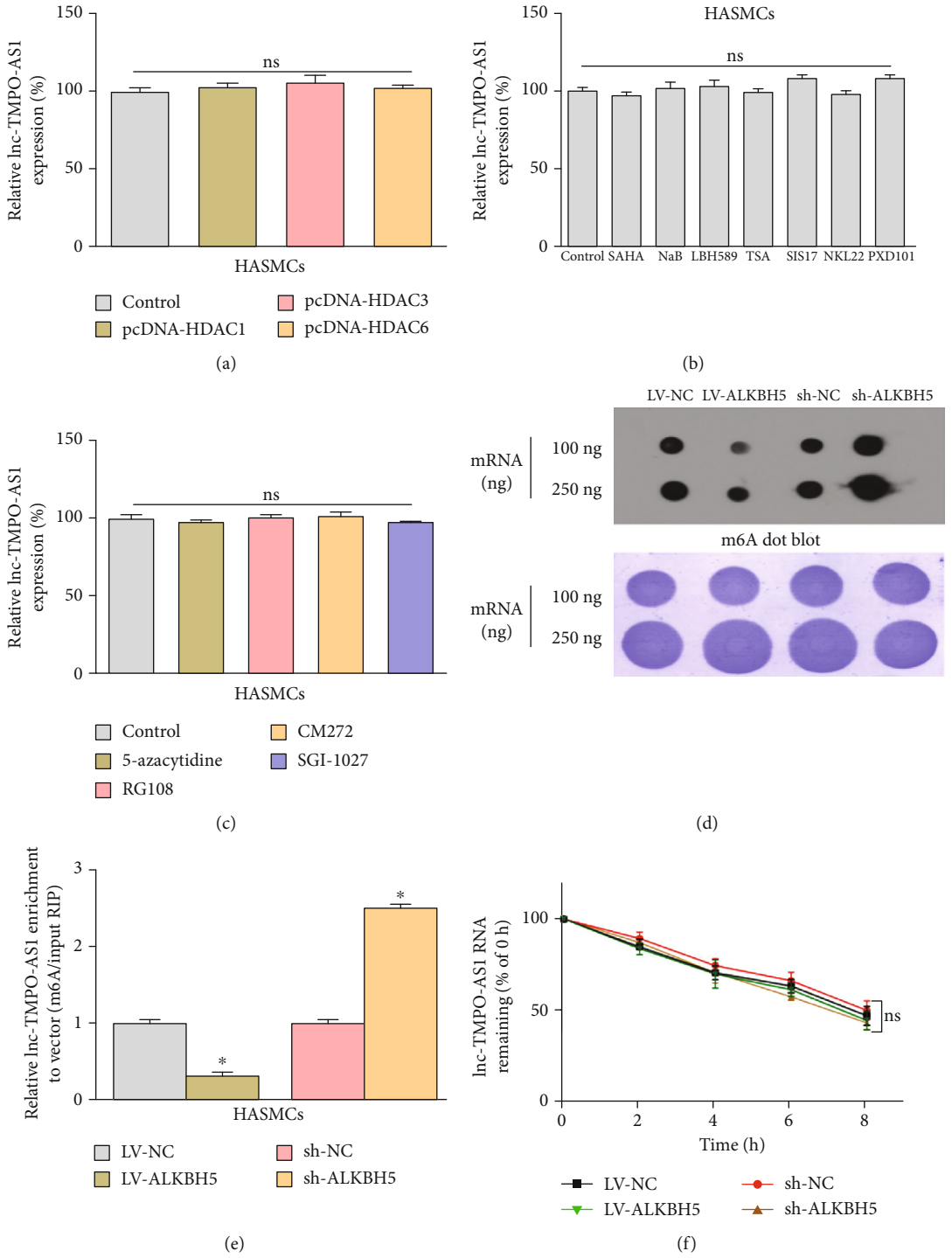

Figure 4: Continued.

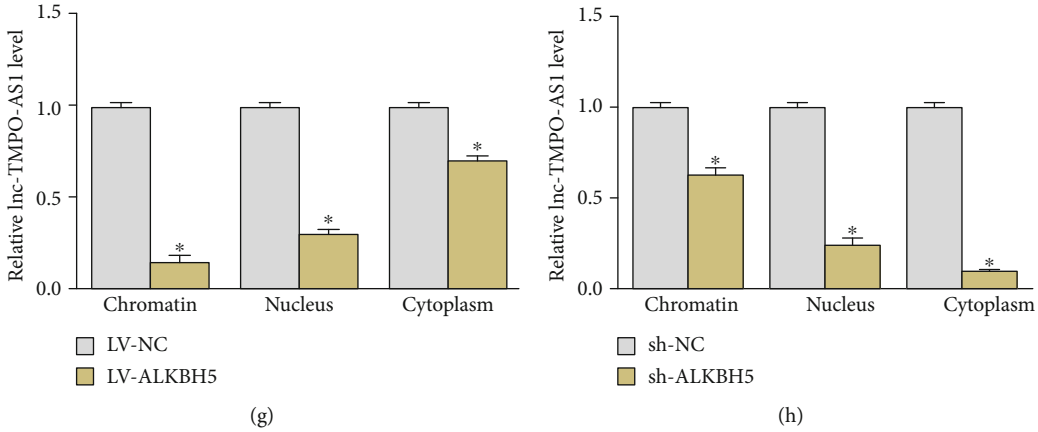

Figure 4: ALKBH5 downregulates lncRNA TMPO-AS1 through m6A demethylation in HASMCs. (a) DNA methylation might not be related to the lnc-TMPO-AS1 expression level in HASMCs. (b, c) Histone acetylation had no significant influence on the lnc-TMPO-AS1 level in HASMCs. (d) M6A dot blot assay revealed that overexpression of ALKBH5 markedly reduced m6A level while silencing ALKBH5 increased this level in HASMCs. (e) M6A RIP-qPCR analysis showed 0.3- and 2.5-fold enrichment in m6A antibody levels of lnc-TMPO-AS1 in ALKBH5-overexpressing and ALKBH5 knockdown cells, respectively. (f) The level changes of ALKBH5 had no significant influence on the half-life of lnc-TMPO-AS1. (g, h) Subcellular fractionation analysis indicated that ALKBH5 overexpression could apparently decrease the localization of lnc-TMPO-AS1 to chromatin while ALKBH5 knockdown enhance its accumulation in chromatin. Data represented the mean ± SEM from three independent experiments, $^*P < 0.05$; ns represents no statistical difference between groups.

3.4. ALKBH5 Downregulates lncRNA TMPO-AS1 through m6A Demethylation in HASMCs. Recent progress in epigenetic regulation has revealed the involvement of m6A modification in various RNAs, including lncRNAs [5–7]. We then wondered whether ALKBH5 also regulated lnc-TMPO-AS1 by m6A modification and therefore began to explore the underlying epigenetic mechanisms responsible for lnc-TMPO-AS1 downregulation. Firstly, to investigate whether DNA methylation was involved in lnc-TMPO-AS1 downregulation, we treated HASMCs with multiple DNA methyltransferase inhibitors, including RG108, CM272, SGI-1027, and 5-azacytidine. Then, their effects on lnc-TMPO-AS1 expression level were examined, whereas no significant results were observed, suggesting that DNA methylation might not be related to the lnc-TMPO-AS1 expression level in HASMCs (Figure 4(a)). Moreover, since it had been previously reported that histone acetylation could regulate lncRNA expression [8, 9], we investigated its role in lnc-TMPO-AS1 expression via treating HASMCs with various histone deacetylase (HDAC) inhibitors, including SAHA, NaB, LBH589, TSA, SIS17, NKL22, and PXD101. The data revealed that these HDAC inhibitors had no significant influence on the lnc-TMPO-AS1 level in HASMCs (Figure 4(b)). This conclusion was further confirmed by results that indicated that overexpression of HDAC, such as HDAC1, HDAC3, and HDAC6, also had no impact on lnc-TMPO-AS1 expression in HASMCs (Figure 4(c)).

Subsequently, to identify whether ALKBH5 depends on m6A demethylation to reduce the expression of lnc-TMPO-AS1 in HASMCs, we first determined the effect of ALKBH5 on m6A level using m6A dot blot assay and found that the overexpression of ALKBH5 markedly reduced m6A level, while silencing ALKBH5 increased this level in HASMCs (Figure 4(d)). Meanwhile, m6A RIP-qPCR analysis showed 0.3- and 2.5-fold enrichment in m6A antibody levels of lnc-TMPO-AS1 in ALKBH5 overexpressing and ALKBH5 knockdown cells, respectively (Figure 4(e)). These data revealed that ALKBH5 downregulates lnc-TMPO-AS1 expression via reducing its m6A level in HASMCs.

We then explored the deeper potential mechanisms associated with the m6A-mediated expression of lnc-TMPO-AS1 in HASMCs. By treating HASMCs with Act-D to terminate transcription, we observed that the level changes of ALKBH5 had no significant influence on the half-life of lnc-TMPO-AS1 (Figure 4(f)). In the following subcellular fractionation analysis, we found that ALKBH5 overexpression could apparently decrease the localization of lnc-TMPO-AS1 to chromatin while ALKBH5 knockdown enhance its accumulation in chromatin (Figures 4(g) and 4(h)), which might be attributed to the cause that ALKBH5 can reduce the stability of nascent lnc-TMPO-AS1. Collectively, these findings indicated that ALKBH5-mediated m6A demethylation is involved in the downregulation of lnc-TMPO-AS1, not by decreasing the stability of its transcript but possibly by decreasing the stability of nascent lnc-TMPO-AS1.

3.5. lncRNA TMPO-AS1 Exhibits Its Biological Roles in HASMCs via Regulating IRAK4. As is well known, lncRNA can regulate gene expression at the epigenetic, transcriptional, or posttranscriptional levels [10]. To elucidate the regulatory role of lnc-TMPO-AS1 in HASMCs, we first screened out genes whose expression was affected by lnc-TMPO-AS1 using an RNA-sequencing analysis. As shown in Figure 5(a), the expression levels of a large number of genes changed significantly after the lnc-TMPO-AS1 knockdown. Subsequently, through extensive literature review, nine of these genes that may be associated with inflammation and apoptosis were selected to validate RNA-seq results. IRAK4 attracted our attention not only because it has been reported as an important molecule in many inflammatory

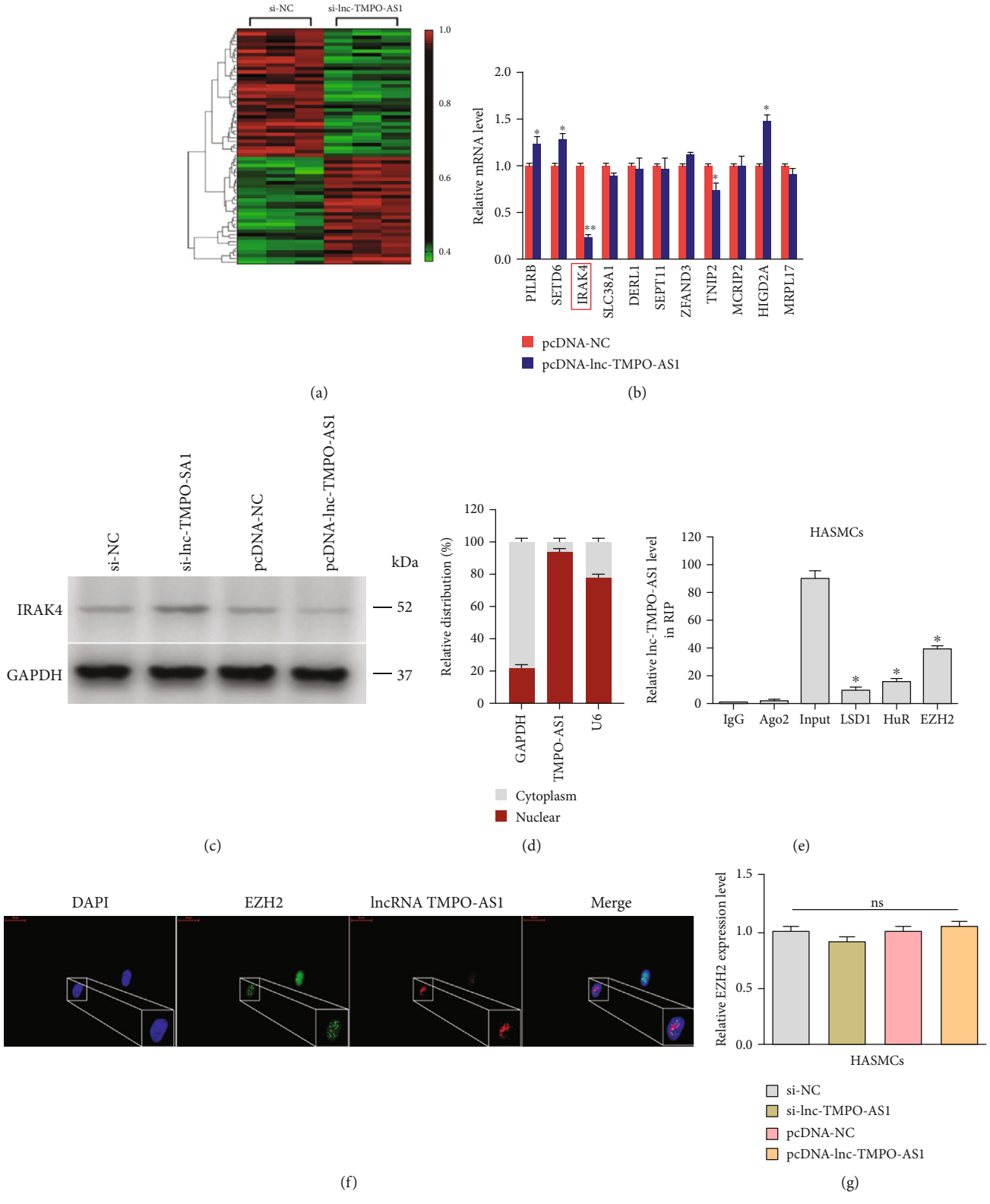

Figure 5: Continued.

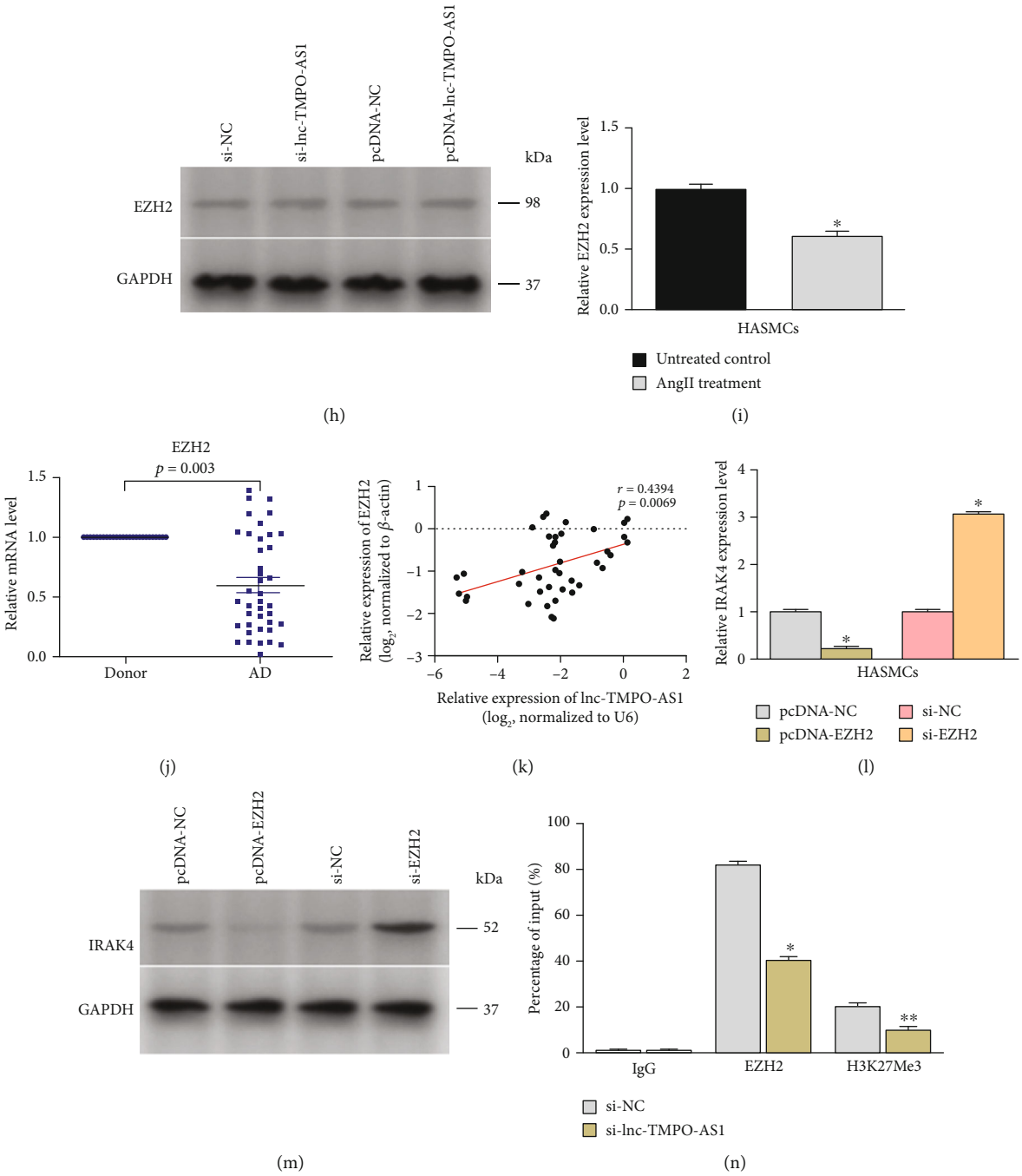

Figure 5: lncRNA TMPO-AS1 exhibits its biological roles in HASMCs via regulating IRAK4. (a) The expression levels of a large number of genes changed significantly after the lnc-TMPO-AS1 knockdown. (b) IRAK4 had the most dramatic expression change when lnc-TMPO-AS1 was overexpressed. (c) The protein level of IRAK4 was negatively regulated by lnc-TMPO-AS1. (d) The result of subcellular fractionation analyses indicated that lnc-TMPO-AS1 was predominantly located in the nucleus. (e) RIP assay revealed that lnc-TMPO-AS1 can combine with HuR, LSD1, and EZH2, with the strongest binding to EZH2. (f) The signals of lnc-TMPO-AS1 and EZH2 were confirmed to be colocalized in HASMCs by FISH and immunofluorescence. (g, h) No significant changes in EZH2 expression appeared in both pcDNA-TMPO-AS1 and si-TMPO-AS1 cells compared to the negative control. (i) EZH2 was downregulated in the AngII treatment group. (j, k) The expression of EZH2 was also reduced in aortas from AD patients and exhibited a positive correlation with lnc-TMPO-AS1 expression ($r = 0.4769$, $P = 0.0339$). (l, m) EZH2 knockdown significantly enhanced the mRNA and protein levels of IRAK4. (n) ChIP assays demonstrated that lnc-TMPO-AS1 knockdown reduced the binding of EZH2 and H3K27Me3 levels at the promoters of IRAK4. Data represented the mean ± SEM from three independent experiments; $^{*}P < 0.05$, $^{**}P < 0.01$.

and apoptotic pathways [11, 12] but also because it had the most dramatic expression change when lnc-TMPO-AS1 was overexpressed (Figure 5(b)). Western blot subsequently confirmed at the protein level that IRAK4 was negatively regulated by lnc-TMPO-AS1 (Figure 5(c) and Supplementary Fig. 8). To elucidate explicitly how lnc-TMPO-AS1

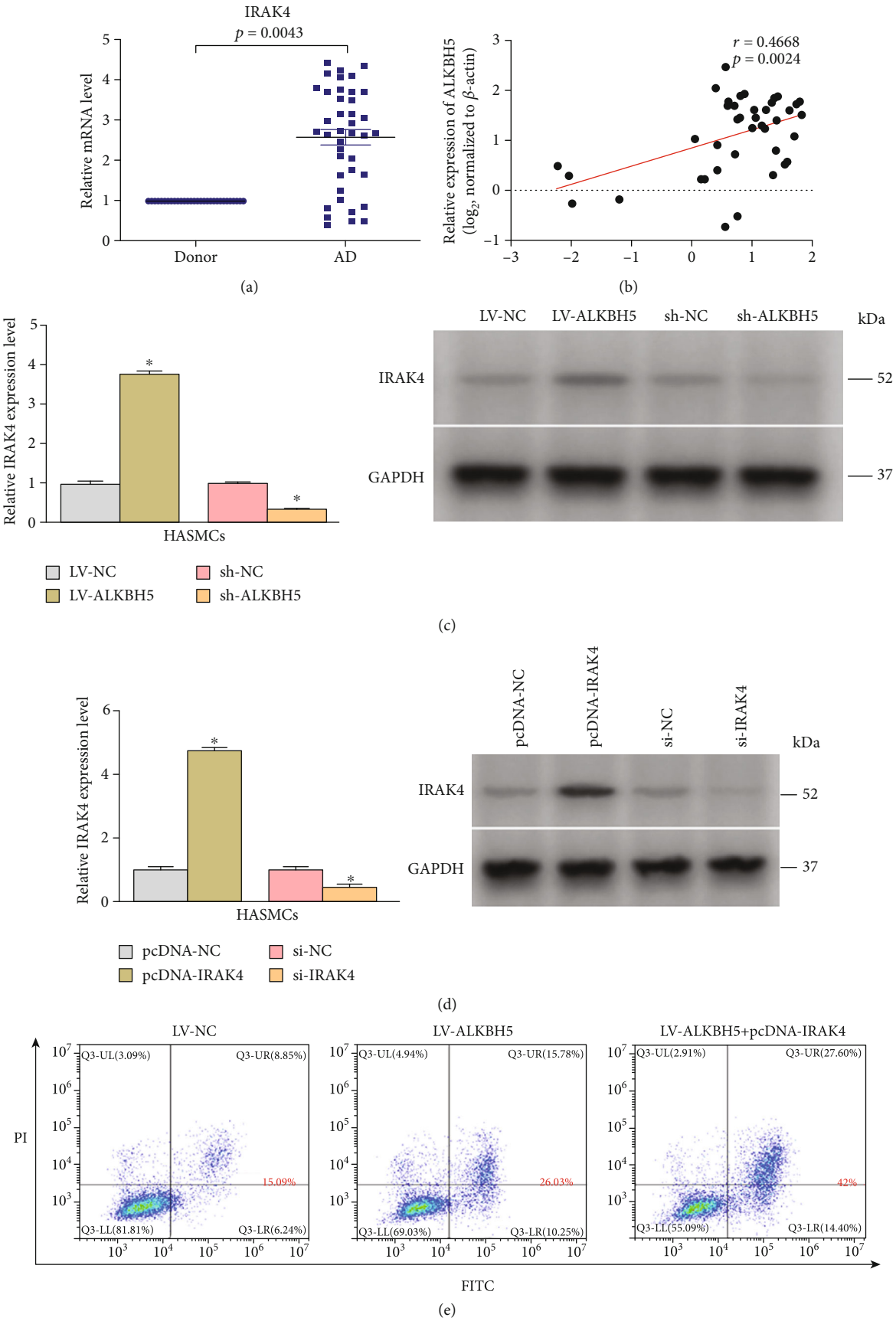

Figure 6: Continued.

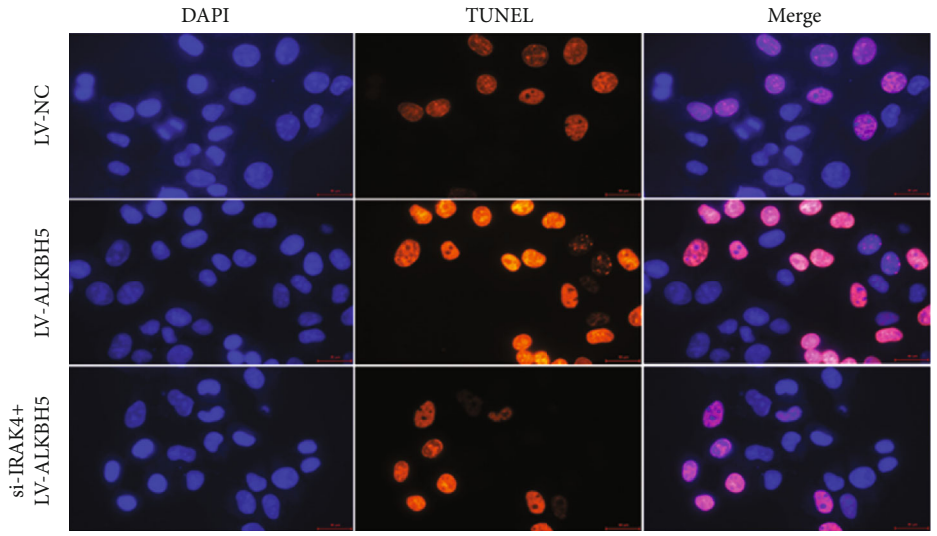

(f)

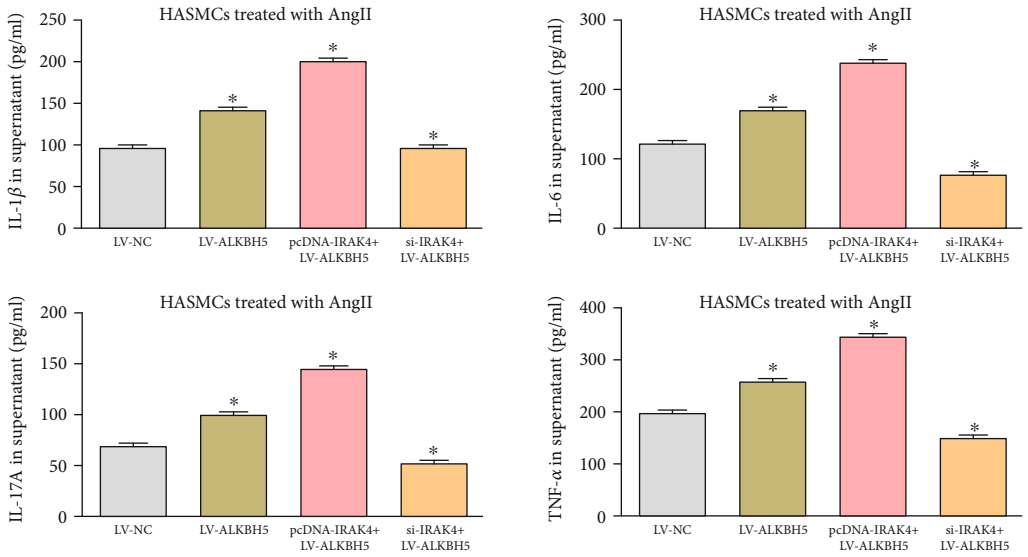

(g)

Figure 6: Continued.

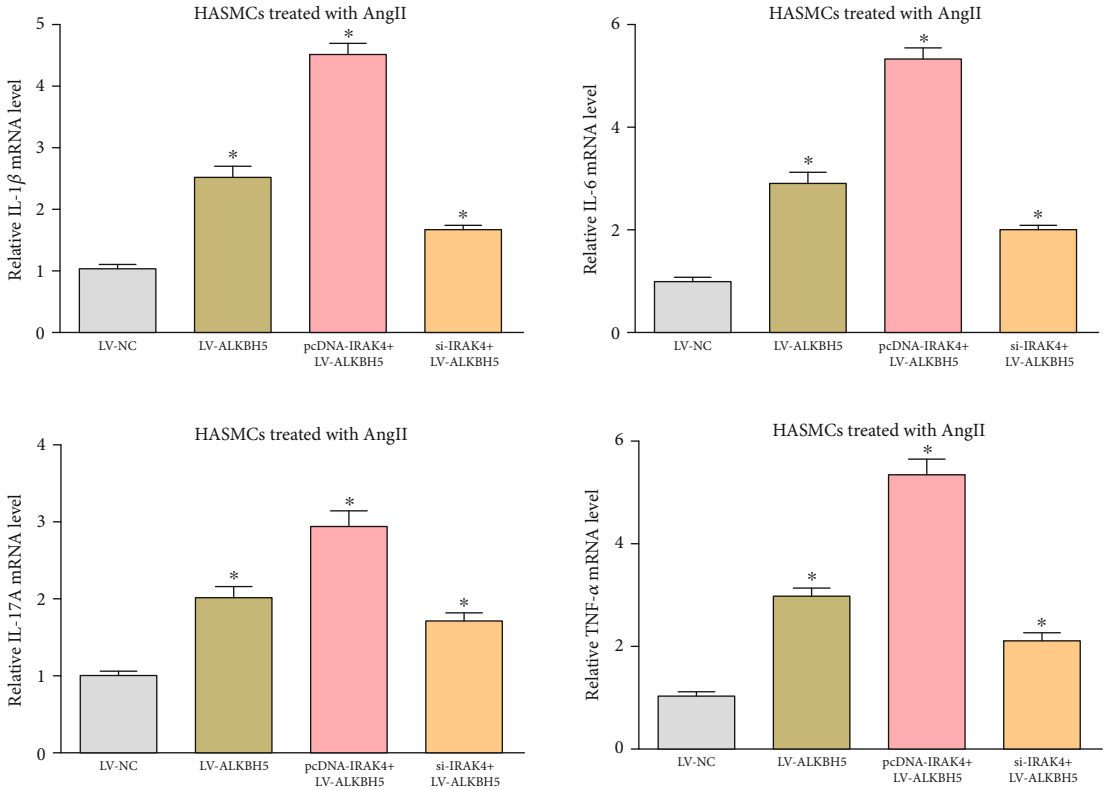

(h)

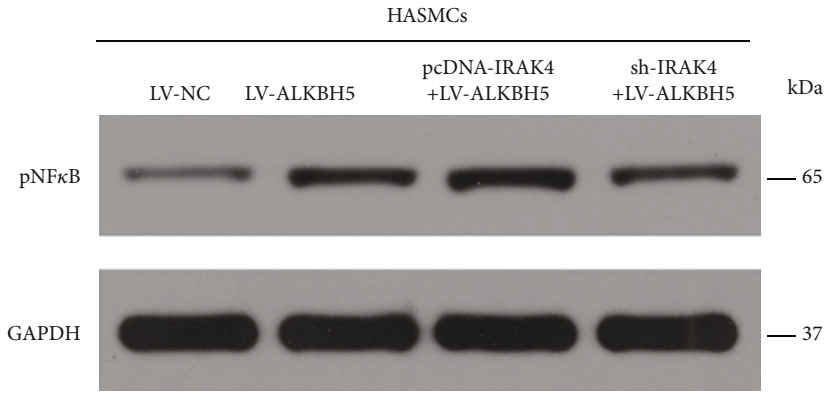

(i)

Figure 6: Continued.

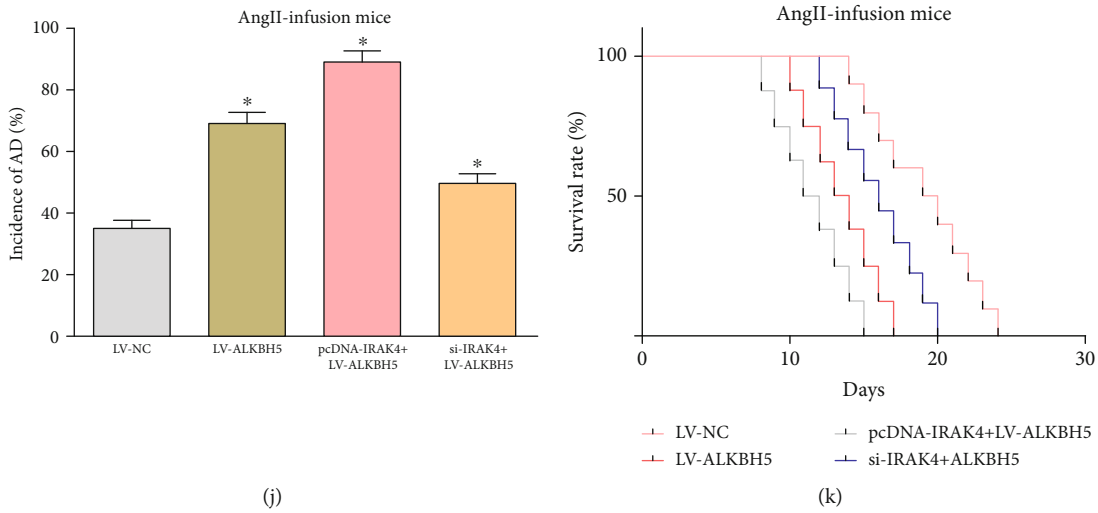

(j) (k)

Figure 6: IRAK4 is positively correlated with ALKBH5 in terms of expression level and biological function. (a, b) The expression level of IRAK4 in 40 pairs of aorta tissues from AD patients and donors was measured and confirmed its negative correlation with ALKBH5 expression by Pearson's correlation coefficient analysis ($r = 0.7048$, $P = 0.0005$). (c) Overexpressing ALKBH5 promoted the expression of IRAK4 while ALKBH5 knockdown suppressed it. (d) The effects of interference on mRNA and protein levels of IRAK4 were confirmed. (e, f) IRAK4 could further promote AngII-induced HASMC apoptosis increased by ALKBH5 overexpression, while IRAK4 knockdown partly counteracted the proapoptotic effect caused by the overexpression of AKLBH5. (g, h) Overexpression of IRAK4 enhanced the hypersecretion of inflammatory cytokines and the high expression of inflammation-related genes caused by ALKBH5 overexpression while silencing IRAK4 could partially offset the proinflammatory effect of ALKBH5. (i) The level of pNFκB was upregulated by ALKBH5, and this effect could be further enhanced by the overexpression of IRAK4 or weakened by its knockdown. (j, k) IRAK4 overexpression or knockdown enhanced or partly offset the influences of ALKBH5 upregulation on the incidence of AD and survival time in mice. Data represented the mean ± SEM from three independent experiments, $^*P < 0.05$.

downregulates IRAK4 in HASMCs, we performed the following mechanistic analysis.

Given that the regulatory function of lncRNA is closely related to its intracellular distribution, we detected the distribution of lnc-TMPO-AS1 in HASMCs using subcellular fractionation analyses. The result indicated that lnc-TMPO-AS1 was predominantly located in the nucleus (Figure 5(d)), suggesting that lnc-TMPO-AS1 may function as a regulator at the epigenetic or transcriptional levels. Previous studies have reported that lncRNA can activate the transcription of its nearby genes in *cis* by promoting chromatin cyclization from transcriptional enhancers [13, 14]. We, therefore, searched the database for the location of lnc-TMPO-AS1 on chromosomes and identified several adjacent transcripts, including RUN4-41P, SNORA53, ADAF1, SLC25A3, IKBIP, ANKS1B, and AC008055.2 (Supplementary Fig. 9). The expression level detection of these genes showed no significant difference between the lnc-TMPO-AS1 overexpression or knockdown group and the control group (Supplementary Fig. 10A–B). Hence, the biological roles of lnc-TMPO-AS1 in HASMCs may not be involved in the *ris* regulatory mechanism.

Recent findings have revealed that lncRNAs can also regulate the expression of downstream genes via interacting with RNA binding proteins (RBPs), such as HuR, LSD1, and EZH2 [15, 16]. To confirm whether lnc-TMPO-AS1 regulates the downstream targets via binding RBPs, RIP was performed and revealed that lnc-TMPO-AS1 can combine with HuR, LSD1, and EZH2, with the strongest binding to EZH2 (Figure 5(e)). Furthermore, as shown in Figure 5(f), the result that signals of lnc-TMPO-AS1 and EZH2 were confirmed to be colocalized in HASMCs by FISH and immunofluorescence, reinforced both the conclusion of the RIP assay (Figure 5(e)) and the results of subcellular fractionation analyses (Figure 5(d)). To further investigate the interaction between lnc-TMPO-AS1 and EZH2, we examined the expression changes of EZH2 after interfering with the level of lnc-TMPO-AS1 and no significant changes appeared in both pcDNA-TMPO-AS1 and si-TMPO-AS1 cells compared to the negative control (Figures 5(g) and 5(h)).

Enhancer of zeste homolog 2- (EZH2-) mediated trimethylation of histone 3 lysine 27 (H3K27Me3) is vital for the negative regulation of immunity intestinal inflammation [17]. To determine whether EZH2 is also involved in the regulation of AngII-induced HASMC inflammation and apoptosis, we first measured the expression level of EZH2 in HASMCs untreated and treated with AngII and observed that EZH2 was downregulated in the treatment group (Figure 5(i)). Consistently, in a subsequent qRT-PCR analysis between AD and normal aorta tissues, the expression of EZH2 was also reduced in aortas from AD patients and exhibited a positive correlation with lnc-TMPO-AS1 expression (Figures 5(j) and 5(k); $r = 0.4769$, $P = 0.0339$). More importantly, we observed that EZH2 knockdown significantly enhanced the mRNA and protein level of IRAK4, while the opposite results occurred when EZH2 was overexpressed (Figures 5(l) and 5(m)). Subsequently, we performed ChIP assays and demonstrated that EZH2 could bind directly to the promoter regions of IRAK4 and cause H3K27 trimethylation (H3K27Me3),

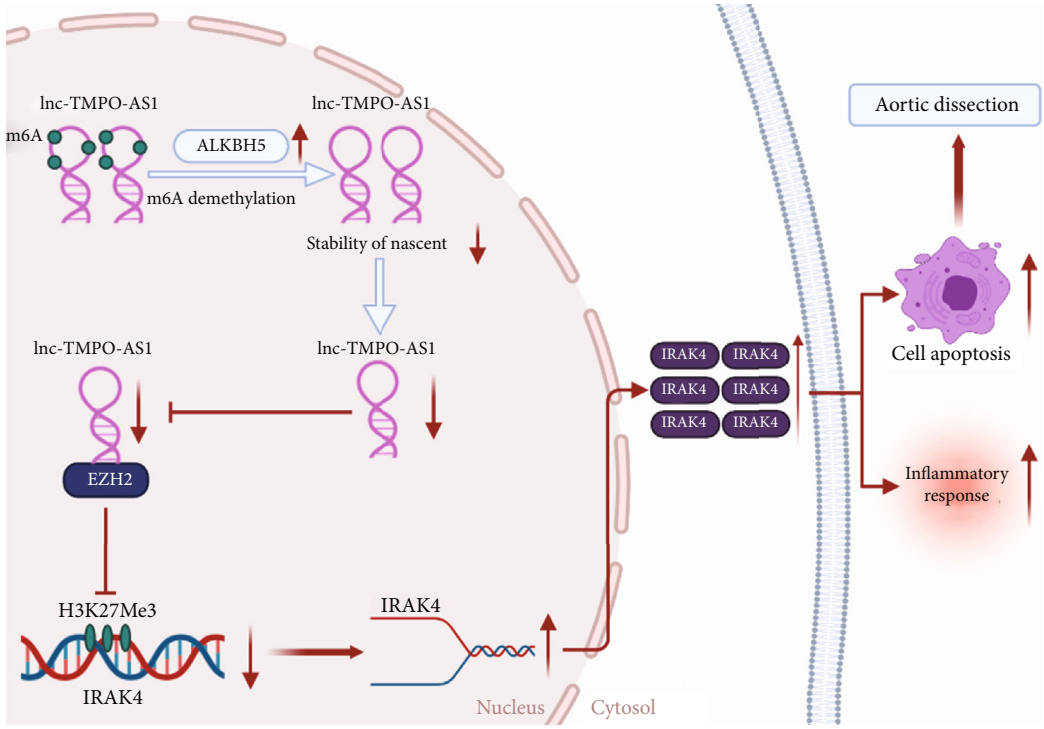

Figure 7: Schematic diagram of the mechanisms revealed in this study. ALKBH5 could aggravate AngII-induced inflammation response as well as apoptosis of HASMCs and increase the incidence of AD in AngII-infused mice through regulating lnc-TMPO-AS1/EZH2/IRAK4 signals in an m6A modification manner.

which results in the suppression of gene expression. Moreover, lnc-TMPO-AS1 knockdown reduced the binding of EZH2 and H3K27Me3 levels at the promoters of IRAK4 (Figure 5(n)). Taken together, these data indicated that lnc-TMPO-AS1 exhibits its functions in AngII-induced HASMC inflammation and apoptosis, at least partly, through downregulating IRAK4 at the epigenetic level by combining with EZH2.

3.6. IRAK4 Is Positively Correlated with ALKBH5 in terms of Expression Level and Biological Function. Since we had elucidated the regulatory relationship between ALKBH5 and lnc-TMPO-AS1, coupled with between lnc-TMPO-AS1 and IRAK4, we next investigated the relationship between ALKBH5 and IRAK4. Firstly, we measured the expression level of IRAK4 in 40 pairs of aorta tissues from AD patients and donors using qRT-PCR and confirmed its negative correlation with ALKBH5 expression by Pearson's correlation coefficient analysis (Figures 6(a) and 6(b); $r = 0.7048$, $P = 0.0005$). To determine whether this negative correlation was due to IRAK4 being regulated by ALKBH5, we detected the expression change of IRAK4 after interfering with ALKBH5. The results revealed that overexpressing ALKBH5 promoted the expression of IRAK4 while ALKBH5 knockdown suppressed it (Figure 6(c)). Furthermore, to explore the relationship between IRAK4 and ALKBH5 in terms of biological function, we elevated the IRAK4 level using pcDNA-IRAK4 or attenuated it with si-IRAK4 in ALKBH5-overexpressing HASMCs and a series of restoration assays were performed. The effects of interference on mRNA and protein levels of IRAK4 were shown in Figure 6(d). Flow cytometry and TUNEL assay revealed that upregulation of IRAK4 could further promote AngII-induced HASMC apoptosis increased by ALKBH5 overexpression, while IRAK4 knockdown partly counteracted the proapoptotic effect caused by the overexpression of AKLBH5 (Figures 6(e) and 6(f) and Supplementary Fig. 11). Consistently, ELISA and qRT-PCR confirmed that the overexpression of IRAK4 enhanced the hypersecretion of inflammatory cytokines and the high expression of inflammation-related genes caused by ALKBH5 overexpression while silencing IRAK4 could partially offset the proinflammatory effect of ALKBH5 (Figures 6(g) and 6(h)). Moreover, we also found that the level of pNFκB was upregulated by ALKBH5 and this effect could be further enhanced by the overexpression of IRAK4 or weakened by its knockdown. (Figure 6(i) and Supplementary Fig. 12). In in vivo experiments, IRAK4 overexpression or knockdown enhanced or partly offset the influences of ALKBH5 upregulation on the incidence of AD and survival time in mice (Figures 6(j) and 6(k)). To sum up, these results identified that IRAK4 is positively correlated with ALKBH5 in terms of expression level and biological function in HAMSCs.

4. Discussion

Nowadays, with the maturation of m6A sequence technology, m6A modification has become a hotspot for research in RNA regulation-related fields [23]. Recently, accumulating evidence has revealed the pivotal roles of m6A modification

in noncoding RNAs in a series of physiological and biochemical processes, including cell proliferation and apoptosis, stem cell self-renewal, fate, and functions of lncRNAs, maturation of pri-miRNA, and RNA-protein interactions [24, 25]. However, most of the above findings are confined to tumor research, and studies in the cardiovascular system remain quite lacking. In this study, our results revealed that ALKBH5, a major m6A demethylase, could exacerbate AngII-induced inflammation damage and apoptosis of HASMCs. As far as we know, this is the first in-depth study on the involvement of ALKBH5 in AD progression through regulating the m6A modification of lncRNAs.

We firstly identified the high expression of ALKBH5, in AD tissues and HASMCs treated with AngII. Then, we demonstrated that ALKBH5 could exacerbate AngII-induced HASMC inflammatory response as well as apoptosis and increase the incidence of AD in AngII-infused mice. Mechanistically, we explored the interrelationship between ALKBH5 and noncoding RNAs and finally identified lncRNA TMPO-AS1 as a downstream signaling target of ALKBH5 in HASMCs. More importantly, we further explored the specific way for ALKBH5 to downregulate lnc-TMPO-AS1 in an m6A modification manner. We first experimentally excluded the involvement of DNA methylation and histone acetylation in this regulatory process and then confirmed that ALKBH5 did not downregulate lnc-TMPO-AS1 though decreasing the stability of its transcript. Finally, we demonstrated that ALKBH5-mediated m6A demethylation is involved in the downregulation of lnc-TMPO-AS1 by decreasing the stability of nascent lnc-TMPO-AS1.

Subsequently, a series of mechanistic studies were conducted to further investigate the downstream effectors of the ALKBH5-lncRNA TMPO-AS1 axis and their regulatory mechanisms. It is well known that lncRNAs are defined as a class of functional noncoding RNA transcripts with more than 200 nucleotides in length and widely engaged in diverse biological processes. Although they cannot directly encode proteins, they can regulate gene expression at various levels, including the epigenetic, transcriptional, posttranscriptional, and translational levels [26]. Given a fact found by subcellular fractionation analyses and FISH assay that lnc-TMPO-AS1 is predominantly distributed in the nucleus of HASMCs, we inferred that lnc-TMPO-AS1 may function as a regulator at the epistatic or transcriptional level. Subsequently, we confirmed that lnc-TMPO-AS1 can directly combine with EZH2, an RNA binding protein, by RIP assay and revealed that EZH2 can bind directly to the promoter regions of IRAK4 and cause H3K27Me3, which leads to the suppression of gene expression through using ChIP assay. To enhance the preciseness of the regulatory pathway in this study, we directly investigated the direct relationship between ALKBH5 and IRAK4, the most downstream effectors in the pathway, in terms of expression level and biological functions and ultimately confirmed the positive correlation between them. Collectively, our data confirm our inference and demonstrated that the ALKBH5-lncRNA TMPO-AS1 axis exhibits its functions in AngII-induced HASMC inflammation and apoptosis, at least partly, through downregulating IRAK4 at the epigenetic level via combining with EZH2.

Despite our best efforts to design and experiment rigorously, the present study still has some limitations. One limitation is that the clinical tissue sample size needs to be further expanded, which could reduce the possibility of bias, such as age bias and gender bias. The main obstacle to obtaining a larger sample size is that normal aorta tissues are derived from donations in China and the number of heart donors declared brain dead is in short supply. Another limitation is that the regulation mechanism of m6A modification on lncRNA expression is still scarce and at the exploratory stage. Therefore, in addition to the regulation manner confirmed in this study, whether ALKBH5 also modulates lnc-TMPO-AS1 in other ways remains to be more comprehensively explored. Moreover, when we look for downstream targets of ALKBH5, we found that lncRNA TMPO-AS1 and MEG3 were remarkably downregulated after ALKBH5 overexpression. Interestingly, however, when ALKBH5 was silenced, only the expression of lncRNA TMPO-AS1 was markedly enhanced, while the level of MEG3 was almost unchanged. The underlying mechanism leading to this interesting phenomenon still needs to be further revealed by subsequent studies.

5. Conclusion

In summary, we demonstrated that ALKBH5 could aggravate AngII-induced inflammation response as well as apoptosis of HASMCs and increase the incidence of AD in AngII-infused mice through regulating lnc-TMPO-AS1/EZH2/IRAK4 signals in an m6A modification manner (Figure 7). Our findings reveal for the first time the role of m6A modification in AD progression and may shed some new light on searching for novel therapeutic approaches to improve the health of patients fighting AD or other cardiovascular diseases.

Data Availability

The data used to support the findings of this study are available from the corresponding author upon request.

Conflicts of Interest

The authors declare that they have no potential conflicts of interest.

Authors' Contributions

Peng Wang and Min Zhang contributed equally to this work. P.W. designed the project plan, completed the main experiment, and drafted the manuscript. Z.W.W. devoted to the resources and supervised the implementation of the whole project. M.Z. organized experimental data and revised the manuscript. Q.W. and F.S. established the AngII-infusion animal model. S.Y. completed the bioinformatics analysis. All authors have read and approved the final version of the manuscript.

Acknowledgments

This work was supported by grants from the National Natural Science Foundation of China (No. 81570428 and No. 81600367), Key Support Project of Health Commission of Hubei Province (No. WJ2019Z012), and Guiding Fund of Renmin Hospital of Wuhan University (No. RMYD2018Z07).

Supplementary Materials

Supplementary Figure 1: quantitative analysis of Figure 1(b) in the main text. Supplementary Figure 2: quantitative analysis of Figure 1(d) in the main text. Supplementary Figure 3: quantitative analysis of Figure 2(k) in the main text. Supplementary Figure 4: quantitative analysis of Figure 2(l) in the main text. Supplementary Figure 5: the interference effects of pcDNA-lnc-TMPO-AS1 and si-lnc-TMPO-AS1 in HASMCs were detected by qRT-PCR. Supplementary Figure 6: quantitative analysis of Figures 3(g) and 3(i) in the main text. Supplementary Figure 7: the effect of lnc-TMPO-AS1 downregulation on the inflammatory response was examined. Supplementary Figure 8: quantitative analysis of Figure 5(c) in the main text. Supplementary Figure 9: the location of lnc-TMPO-AS1 on chromosomes and several adjacent transcripts were identified. Supplementary Figure 10: the expression of some genes whose transcripts are close to lnc-TMPO-AS1 on chromosomes. Supplementary Figure 11: quantitative analysis of Figure 6(f) in the main text. Supplementary Figure 12: quantitative analysis of Figure 6(i) in the main text. *(Supplementary Materials)*

References

[1] C. A. Nienaber, R. E. Clough, N. Sakalihasan et al., "Correction: aortic dissection," *Nature Reviews. Disease Primers*, vol. 2, no. 1, p. 16071, 2016.

[2] J. Gawinecka, F. Schnrath, and A. von Eckardstein, "Acute aortic dissection: pathogenesis, risk factors and diagnosis," *Swiss Medical Weekly*, vol. 147, p. w14489, 2017.

[3] A. Karimi and D. M. Milewicz, "Structure of the elastin-contractile units in the thoracic aorta and how genes that cause thoracic aortic aneurysms and dissections disrupt this structure," *The Canadian Journal of Cardiology*, vol. 32, no. 1, pp. 26–34, 2016.

[4] D. M. Milewicz, S. K. Prakash, and F. Ramirez, "Therapeutics targeting drivers of thoracic aortic aneurysms and acute aortic dissections: insights from predisposing genes and mouse models," *Annual Review of Medicine*, vol. 68, no. 1, pp. 51–67, 2017.

[5] D. M. Milewicz, K. M. Trybus, D. C. Guo et al., "Altered smooth muscle cell force generation as a driver of thoracic aortic aneurysms and dissections," *Arteriosclerosis, Thrombosis, and Vascular Biology*, vol. 37, no. 1, pp. 26–34, 2017.

[6] W. Ren, Z. Wang, J. Wang et al., "IL-5 overexpression attenuates aortic dissection by reducing inflammation and smooth muscle cell apoptosis," *Life Sciences*, vol. 241, p. 117144, 2020.

[7] S. L. Berger, "Histone modifications in transcriptional regulation," *Current Opinion in Genetics & Development*, vol. 12, no. 2, pp. 142–148, 2002.

[8] H. Akhavan-Niaki and A. A. Samadani, "DNA methylation and cancer development: molecular mechanism," *Cell Biochemistry and Biophysics*, vol. 67, no. 2, pp. 501–513, 2013.

[9] W. A. Cantara, P. F. Crain, J. Rozenski et al., "The RNA modification database, RNAMDB: 2011 update," *Nucleic Acids Research*, vol. 39, no. Database issue, pp. D195–D201, 2010.

[10] R. Desrosiers, K. Friderici, and F. Rottman, "Identification of methylated nucleosides in messenger RNA from Novikoff hepatoma cells," *Proceedings of the National Academy of Sciences of the United States of America*, vol. 71, no. 10, pp. 3971–3975, 1974.

[11] K. D. Meyer, Y. Saletore, P. Zumbo, O. Elemento, C. E. Mason, and S. R. Jaffrey, "Comprehensive analysis of mRNA methylation reveals enrichment in 3′ UTRs and near stop codons," *Cell*, vol. 149, no. 7, pp. 1635–1646, 2012.

[12] D. Dominissini, S. Moshitch-Moshkovitz, S. Schwartz et al., "Topology of the human and mouse m^6A RNA methylomes revealed by m^6A-seq," *Nature*, vol. 485, no. 7397, pp. 201–206, 2012.

[13] H. Song, X. Feng, H. Zhang et al., "METTL3 and ALKBH5 oppositely regulate m6A modification ofTFEBmRNA, which dictates the fate of hypoxia/reoxygenation-treated cardiomyocytes," *Autophagy*, vol. 15, no. 8, pp. 1419–1437, 2019.

[14] I. A. Roundtree, M. E. Evans, T. Pan, and C. He, "Dynamic RNA modifications in gene expression regulation," *Cell*, vol. 169, no. 7, pp. 1187–1200, 2017.

[15] S. Lin, J. Choe, P. Du, R. Triboulet, and R. I. Gregory, "The m^6A methyltransferase METTL3 promotes translation in human cancer cells," *Molecular Cell*, vol. 62, no. 3, pp. 335–345, 2016.

[16] T. Lan, H. Li, D. Zhang et al., "KIAA1429 contributes to liver cancer progression through N6-methyladenosine-dependent post-transcriptional modification of GATA3," *Molecular Cancer*, vol. 18, no. 1, p. 186, 2019.

[17] J. Zhang, S. Guo, H. Y. Piao et al., "ALKBH5 promotes invasion and metastasis of gastric cancer by decreasing methylation of the lncRNA NEAT1," *Journal of Physiology and Biochemistry*, vol. 75, no. 3, pp. 379–389, 2019.

[18] P. Wang, Z. Wang, M. Zhang, Q. Wu, and F. Shi, "Lnc-OIP5-AS1 exacerbates aorta wall injury during the development of aortic dissection through upregulating TUB via sponging miR-143-3p," *Life Sciences*, vol. 271, p. 119199, 2021.

[19] W. Liu, B. Wang, T. Wang et al., "Ursodeoxycholic acid attenuates acute aortic dissection formation in angiotensin II-infused apolipoprotein E-deficient mice associated with reduced ROS and increased Nrf2 levels," *Cellular Physiology and Biochemistry*, vol. 38, no. 4, pp. 1391–1405, 2016.

[20] P. Wang, Y. Deng, and X. Fu, "miR-509-5p suppresses the proliferation, migration, and invasion of non-small cell lung cancer by targeting YWHAG," *Biochemical and Biophysical Research Communications*, vol. 482, no. 4, pp. 935–941, 2017.

[21] Q. Wu, J. Hong, Z. Wang et al., "Abnormal ribosome biogenesis partly induced p53-dependent aortic medial smooth muscle cell apoptosis and oxidative stress," *Oxidative Medicine and Cellular Longevity*, vol. 2019, Article ID 7064319, 19 pages, 2019.

[22] S. Mitchell, J. Vargas, and A. Hoffmann, "Signaling via the NFκB system," *Wiley Interdisciplinary Reviews. Systems Biology and Medicine*, vol. 8, no. 3, pp. 227–241, 2016.

[23] J. Cai, Z. Chen, J. Wang et al., "circHECTD1 facilitates glutaminolysis to promote gastric cancer progression by targeting

miR-1256 and activating β-catenin/c-Myc signaling," *Cell Death & Disease*, vol. 10, no. 8, p. 576, 2019.

[24] Y. Fu, D. Dominissini, G. Rechavi, and C. He, "Gene expression regulation mediated through reversible m^6A RNA methylation," *Nature Reviews. Genetics*, vol. 15, no. 5, pp. 293–306, 2014.

[25] G. Cao, H.-B. Li, Z. Yin, and R. A. Flavell, "Recent advances in dynamic m6A RNA modification," *Open Biology*, vol. 6, no. 4, article 160003, 2016.

[26] F. Kopp and J. T. Mendell, "Functional classification and experimental dissection of long noncoding RNAs," *Cell*, vol. 172, no. 3, pp. 393–407, 2018.